SHRP-S/FR-92-105

Condition Evaluation of Concrete Bridges Relative to Reinforcement Corrosion

Volume 3: Method for Evaluating the Condition of Asphalt-Covered Decks

Anthony J. Alongi
Penetradar Corporation
Niagara Falls, NY

Gerardo G. Clemena
Virginia Transportation Research Council
Charlottesville, VA 22903

Philip D. Cady
Pennsylvania Transportation Institute
The Pennsylvania State University
University Park, PA

Strategic Highway Research Program
National Research Council
Washington, DC 1992

SHRP-S/FR-92-105
ISBN: 309-05259-0
Contract C-101

Program Manager: *Don M. Harriott*
Project Manager: *Joseph F. Lamond*
Copy Editor: *Katharyn Bine Brosseau*
PTI Technical Editor: *Joanne M. Fox*
Program Area Secretary: *Ann Saccomano*

September 1992

Key words:
asphalt-covered decks
bridge decks
delaminations
ground-penetrating radar
nondestructive testing
radar

Strategic Highway Research Program
2101 Constitution Avenue N.W.
Washington, DC 20418

(202) 334-3774

Acknowledgments

The research described herein was supported by the Strategic Highway Research Program (SHRP). SHRP is a unit of the National Research Council that was authorized by Section 128 of the Surface Transportation and Uniform Relocation Assistance Act of 1987.

The authors wish to acknowledge the assistance of officials in the Departments of Transportation of Virginia, New York, and Vermont regarding the selection and testing of bridge decks in their respective states.

Special thanks are due Mr. Ronald I. Frascoia of the Vermont Agency of Transportation and Mr. Frederick Szczepanek of the New York State Department of Transportation.

Contents

List of Figures

List of Tables

Abstract

State highway agencies need a nonintrusive means of evaluating the condition of asphalt-covered concrete bridge decks for reinforcement corrosion. Information on the condition of the concrete deck is needed in order to estimate service life, to program rehabilitation and maintenance activities, and to estimate quantities for rehabilitation contracts. This volume describes the development of a technique for nondestructively determining the presence of delaminations at the top and bottom reinforcement levels. The technique employs the use of short pulse, ground-penetrating radar.

Extensive radio frequency (RF) modeling of the bridge deck scenario was carried out in order to establish theoretical limits of parameters and capabilities. Field testing 22 bridges in Virginia, New York, and Vermont provided the empirical data for the evaluation of various deterioration discriminants in order to identify those providing optimum prediction capabilities. Ground truth data in the form of cores (in the cases where the asphaltic concrete was subsequently removed for repair purposes), chain drag sounding, and actual repair areas were also collected on the bridge sites. The best discriminant for delamination at the top reinforcement level is signal attenuation, and at the bottom reinforcement level, increase in the amplitude of the bottom rebar signal.

Advanced radar data acquisition and signal processing equipment and software were also developed to provide a useable system at the practical level.

Executive Summary

The objective of this research was to develop a means to nondestructively evaluate the condition of asphalt-covered bridge decks. The condition of the concrete is especially critical where the asphalt overlay occurs directly on the concrete deck, i.e., without the use of a waterproof membrane. This is often done to provide an acceptable traffic surface on a deck that has spalled due to reinforcement corrosion. The asphalt overlay often acts as a sponge, holding salt-laden water and accelerating the corrosion of the reinforcement. Therefore, it is important to be able to detect the extent of damage due to reinforcement corrosion in order to estimate remaining service life, to program rehabilitation and maintenance activities, and to estimate quantities for rehabilitation contracts.

This report covers the development of a procedure and attendant facilities to nondestructively determine the presence of delaminations produced by corroding reinforcement in asphalt-covered bridge decks using short pulse, ground-penetrating radar. Advanced radar data acquisition and signal processing equipment and software were developed in order to provide a workable system that can be operated by technician-level personnel.

An analytical computer model and algorithm for radar interaction with the multilayered bridge deck system was developed and used with bench scale experiments to test the capabilities and define the limits of this application of radar technology. From these experiments it was determined that radar can detect the delamination gap directly when the concrete is dry and power losses are low, and that under high loss conditions, detection by radar is possible by measurement of a signal attenuation discriminant.

Using radar and ground truth data from 22 bridge decks in Virginia, New York, and Vermont, radar discriminants were evaluated. The optimum deterioration discriminants for delamination at the top reinforcing steel (signal attenuation) and the bottom reinforcing steel (increase in the amplitude of the bottom reinforcement signal) were identified. The optimum signal attenuation threshold for delamination at the top steel was also established. The ground truth in this experimentation consisted of cores and, in cases where the asphaltic

concrete was subsequently removed for repair purposes, chain drag sounding and actual repair volumes.

A test method procedure, in American Society of Testing and Materials format, has been prepared and appears in Volume 8, "Procedure Manual," of this report.

1

Introduction

Needs

Cost-effective bridge deck rehabilitation makes it necessary to accurately estimate the quantity of deteriorated concrete in a bridge deck, locate these areas for removal, and then effect repair. The primary step in this process is the accurate estimation of repair quantities. Problems exist, however, relative to the use of conventional destructive and nondestructive methods for this purpose on asphalt-covered bridge decks. Conventional nondestructive test methods, such as hammer and chain drag, do not fare well on asphalt-covered decks as a result of inefficient coupling of energy between the asphalt and concrete. Therefore, these techniques are only used just prior to rehabilitation for locating deteriorated areas after asphalt has been removed. Destructive methods such as core samples are effective only when large numbers of random samples are obtained. This is both costly and unnecessarily damaging to the bridge deck.

From the bridge engineer's standpoint, the major concerns with respect to bridge deck deterioration are the forms of deterioration that impair the structural load-carrying capacity of the bridge deck or the rideability of the pavement. One type of deterioration, delamination of the concrete at the level of reinforcing steel, falls into this category. Concrete delamination is the result of corrosion of the reinforcing steel causing a laminar separation or fracture plane to develop.

Objective

The goal of this research is to develop a method that is usable by the State highway departments to detect concrete deterioration and estimate repair quantities on bridge decks covered with an asphalt wearing course.

Scope

The specific objectives of this effort were:

1. The development of the selected nondestructive technology by better defining its abilities relative to the detection of both top- and bottom-level bridge deck delaminations;

2. Improving the system in a manner such that it could be utilized effectively by state highway agencies for detections; and

3. Estimation of deterioration quantity in bridge decks with asphalt overlays, either directly with state highway department personnel or through engagement of consultants.

2

Background and Research Approach

Method Selection

Short pulse, ground-penetrating radar (GPR) was selected for investigation because its noncontacting ability to penetrate asphalt overlays and potential for widespread use by state transportation departments for bridge deck inspection applications. Previous studies have shown that radar may be a practical tool for nondestructive inspection and evaluation of asphalt-covered bridge decks (1-8). Two other methods, infrared thermography and impact echo, were also considered. These methods were rejected because of their inability to meet requirements relating to noncontacting, nondestructive detection or their ineffectiveness and reported unreliability when used on bridge decks with asphalt overlays (*5,6*).

Principles of GPR

Short pulse GPR is a unique type of radar design based on the necessary tradeoff between propagation depth through solid, nonmetallic materials and resolution in the medium (9). In its current form, this type of radar has the performance capability to "look" through several inches of asphalt and concrete with the necessary resolution to distinguish the typical material layers and components of the bridge deck in most cases. Radar propagation in a solid medium is analogous to acoustic sounding inasmuch as echoes or reflections originate at the interface of differing materials. In the case of radar, echoes are produced at the interface of materials with different dielectric properties. Figure 2-1 shows the Model PS-24 Penetradar short pulse radar, which was utilized throughout this project.

Figure 2-1. Penetradar short pulse GPR.

Short pulse GPR operates in a manner similar to conventional radar except that the propagation medium is a solid (asphalt or portland cement concrete), and the scan range is considerably reduced. These requirements, however, place very strict constraints on system and component design in order to function in the required manner.

Typically, a short pulse GPR emits a precisely timed, very short pulse of low-power, radio frequency (RF) energy. Each pulse of RF energy is about one nanosecond (ns) in duration and occurs at a rate greater than one million times per second. The transmitted pulse is radiated downward by the radar antenna into the bridge deck. A portion of the RF energy is reflected wherever there is a change or discontinuity in the dielectric properties of the media. The remaining energy propogates through the boundary. The amplitude of the signal reflected from and through the boundary depends on the relative dielectric difference between the materials at the boundary. RF reflections or radar target echoes are picked up by the antenna, coupled into the receiver, and processed for display, recording, and deterioration detection.

The time from transmission to reception of an echo is referred to as the transit time through a material. In free space or air a radar pulse will travel 11.8 in. (30 cm) in 1 ns. In solid materials the velocity of propagation is reduced. Therefore, the transit time of a radar pulse to or from an object is directly related to its depth and the medium through which it propagates. The radar return waveform consists of echoes from the surface, followed by subsurface reflections. For asphalt-covered bridge decks, the reflection from the deck surface is followed by an echo from the asphalt to concrete interface (A/C echo), the echo from the top and bottom reinforcing steel, and from the bottom of the bridge deck, as shown in Figure 2-2.

Research Approach

The approach that was employed to determine the capability of GPR in the detection of deterioration in asphalt-covered bridge decks involved a comprehensive program consisting of bridge deck field tests, analytical RF modeling of concrete deterioration, and laboratory investigations.

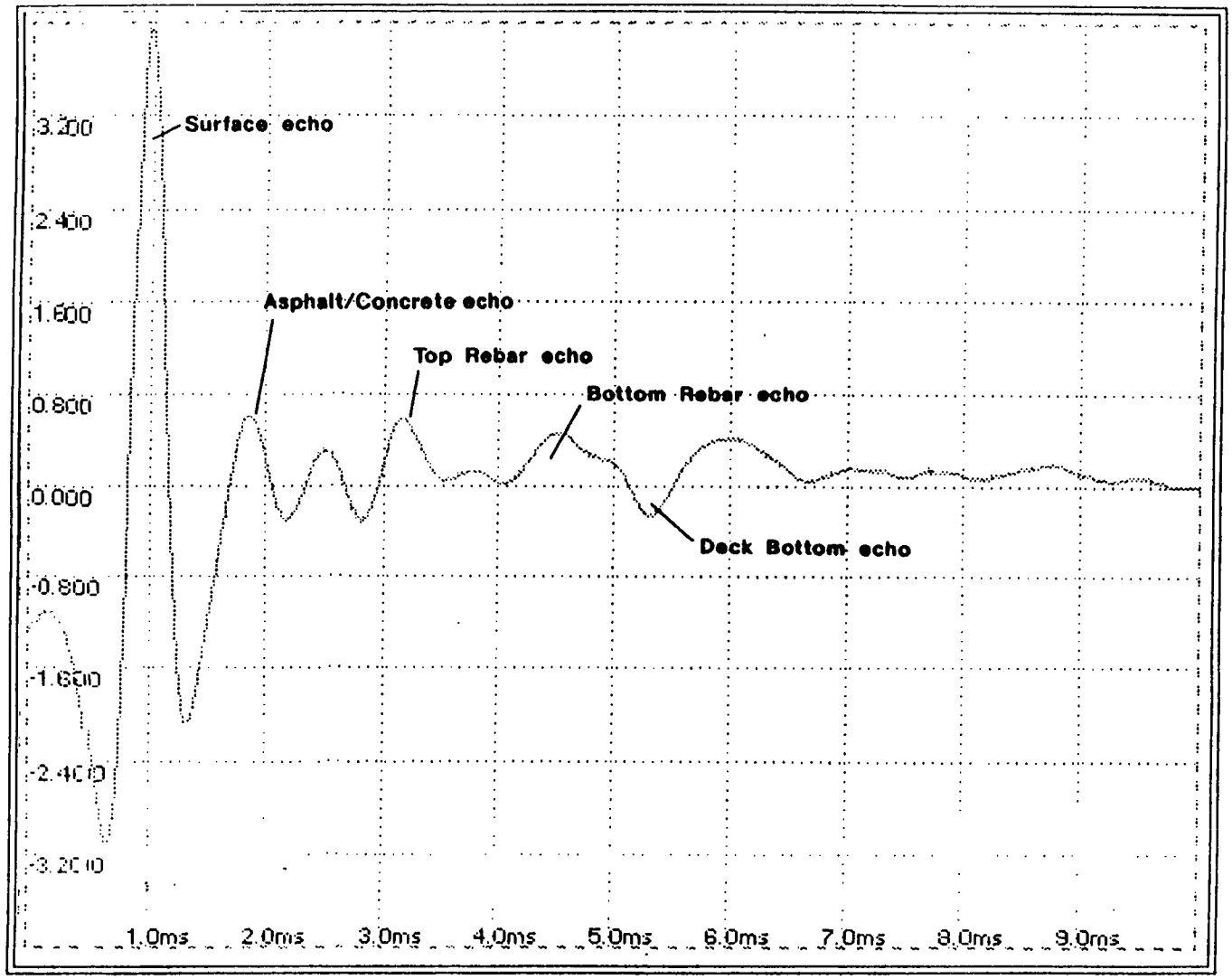

Figure 2-2. Typical radar return waveform from asphalt-covered bridge deck.

The experimental approach necessitated the acquisition of radar data from several sample bridge decks while taking into consideration different geographical locations and climatic conditions. Throughout the project, radar data were gathered from a relatively large number of individual bridge decks in order to ensure a representative sampling. The radar data from these decks were observed and analyzed for unique signal variations in the radar waveform and compared with ground truth data to identify unique delamination discriminants. Once prospective delamination discriminants were identified, a model was developed to analytically describe this interaction of the RF signal with the propagation medium. Based on this, additional analytical studies as well as field and laboratory experiments were designed and conducted to validate and quantify the model. Using the results of the field and laboratory tests, an analytical evaluation was performed to determine the most effective delamination discriminant. Finally, the detection threshold for the selected indicator was empirically determined whereby accurate repair quantity predictions could be made using the radar results. Concurrent with the work on bridge deck deterioration detection, improved hardware and software were developed for computer acquisition of radar waveforms and processing of delamination signals.

3

Equipment and Software Development

Hardware Development

A problem related to the use of radar in bridge deck inspection has been in dealing with the large quantities of data generated. For example, a single Penetradar radar unit will generate range scans (wave forms) at a rate of 50 per second. In 1 hour of operation 180,000 scans will be produced. Conventional recording of these signals has been limited to FM instrumentation recorders, which were capable of handling this magnitude of data, in an analog manner. With the advent of high-speed microcomputer technology, it was possible to develop a system to handle these large data volumes at the prevailing data rates of the radar. One objective of this project was the development of a computer-based system for real-time digital data acquisition and high-speed processing of radar signals. A data acquisition system was designed around the Penetradar Model PS-24 radar, which was capable of direct digitization of radar waveforms, recording of distance and locational information, and providing storage of this data on hard disk for subsequent processing. Furthermore, the system was developed with the capability of handling the output of three radar systems operating at their maximum data rate, simultaneously. The system developed consisted of a digitizing subsystem, disk storage system, computer interface unit, and PC-based microcomputer. Figure 3-1 shows the system schematically in functional block diagram form.

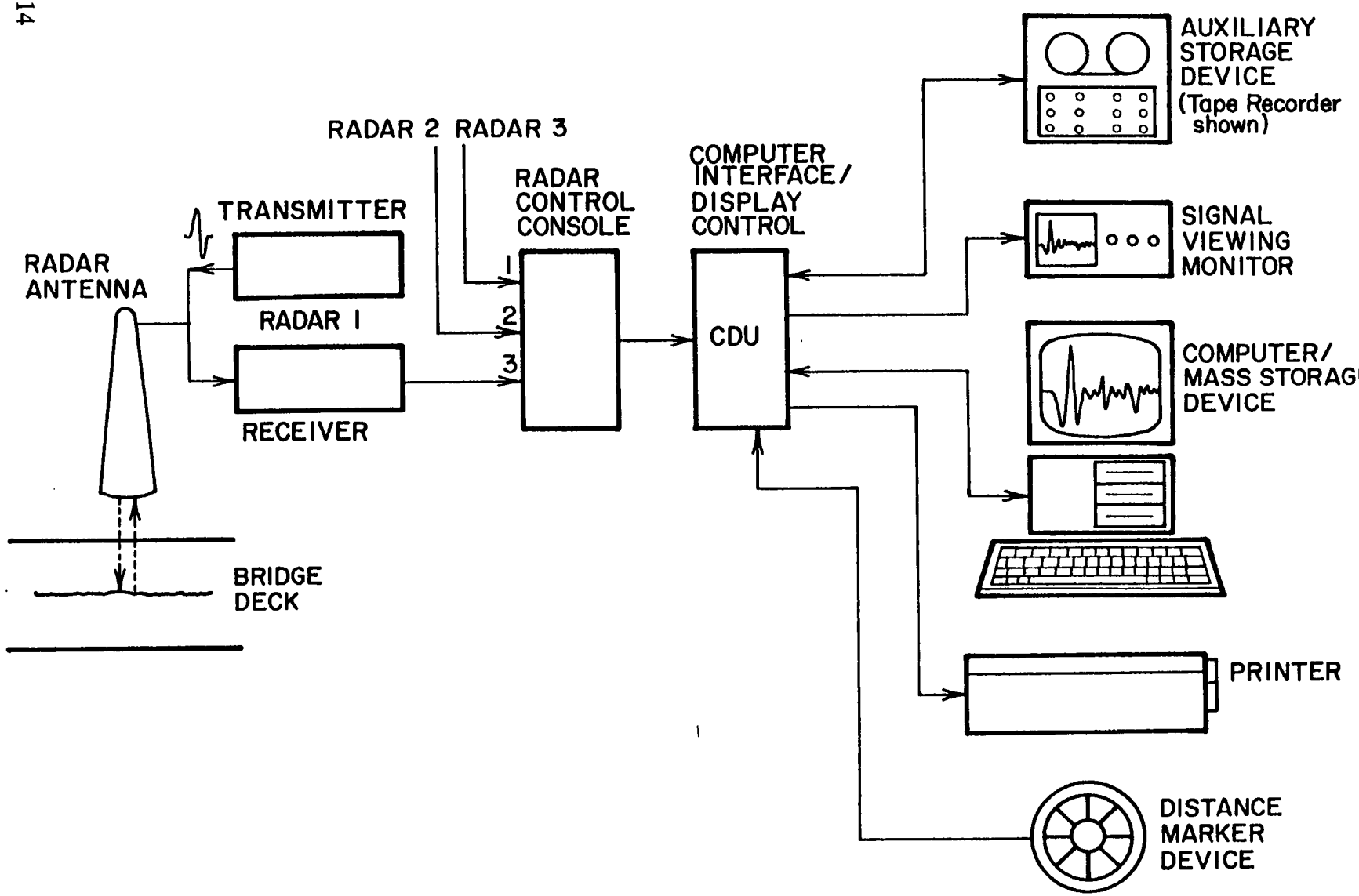

Figure 3-1. Functional block diagram for the radar and support equipment.

In order to estimate the requirements of the digitizing subsystem, the radar system parameters were first defined. The radar emits transmitted signals at very high rates, over one million times per second. After a time-scaling process, the radar signals are decreased in bandwidth to approximately 2.5 kHz. With a radar range sweep rate of 50 Hz, the sampling rate of a digitizing system can be defined. Assume that a factor of 10 times the Nyquist sampling criteria is acceptable for accurate peak location of signals. This suggests that a sampling rate of 50 kHz is necessary. For simultaneous digitization of three radars in parallel, the overall data rate of the acquisition subsystem would need to be 150 kHz. The resolution of the digitizing subsystem is a function of the dynamic range of the radar system itself. The dynamic range of the Penetradar radar is in excess of 60 dB. Therefore, the analog to digital conversion resolution must exceed 10 bits. A resolution of 12 bits was selected.

A storage device was necessary such that large quantities of data could be saved for future processing. In order to calculate the size of such a device, certain parameters had to be defined, including the minimum longitudinal distance resolution between stored waveforms and the maximum storage distance. If it is desired that waveforms be stored at 6-in. (15.2 cm) intervals and the maximum continuous inspection distance is 1/2 mi, then a total of 15,840 waveforms would be digitized in this distance. If we use the previously defined sampling rate, we can determine the total data quantity in this distance. At a rate of 50 kHz, each waveform would have 1,000 sample points. The radar dynamic range is in excess of 60 dB, so an 8-bit conversion (48 dB) is insufficient. Therefore, at least a 10-bit digitization is required for 60 dB, meaning that 2 bytes per sample point must be stored. At 2,000 bytes per waveform (1,000 sample points x 2 bytes per point) the total requirement per 1/2 mi of data is 31.68 MB for three radars. It is rare that more than 5 pass mi of radar data would be taken on a single bridge deck at any one time before stopping. Therefore, a 330-MB shock-mounted hard disk was selected for data storage. Once the disk was filled, the data were transferred to a 1/4-in. tape backup device.

The microcomputer was selected in accordance with the following criteria:

- Speed: the computer must be fast enough to acquire data at a full acquisition bandwidth of 150 kHz; and

- Addressable memory: the computer must be able to address at least 32 MB of memory.

The computer system that was assembled was built around a 33 MHz 80486 ISA PC motherboard, with up to 64 addressable MB of RAM memory, but installed with 32 MB onboard. A rack-mountable industrial computer system was built as shown in Figure 3-2. A special device was designed and built to provide an interface capability between the radars, the display oscilloscope, and the computer system. This unit was designated as the Computer Interface and Display Control Unit (CDU) and served as a centralized point of control and connection between each of the other units. The CDU is used to monitor the inspection distance and speed, and for control between computer and display or radar and display. It also provides all necessary synchronization signals for the control of data digitization (A/D) and reconstruction of data (D/A). The CDU was constructed as both a rack mountable unit and a portable unit for laboratory use. These units are shown in Figures 3-3 and 3-4.

Software Development

Data acquisition and signal processing software was developed to accompany the previously described equipment. The acquisition software was written in C language, as a user friendly, menu-based package for high-speed acquisition of radar data from the Penetradar short pulse radar. This software consists of four components: data acquisition, data review to computer monitor, data review to oscilloscope, and calibration for signal enhancement. The data acquisition mode provides flexibility to the user. It allows variation of acquisition parameters depending on application (such as sampling rate, sampling time, and selection of the number of radar and radar signals to be digitized). It displays the maximum possible acquisition distance based on user parameter selections. A data header file precedes the actual radar data and contains parameter selections as well as user comments, test site information, initial reference locations, and other related information. Raw radar data files are generated in a binary format that is compatible with signal-processing software. Previously digitized radar data can be displayed on either an oscilloscope or a computer monitor along with location information. For display on the computer monitor, the waveform review speed may be changed dynamically or completely halted for detailed examination. Cursors in the X and Y plane (time and amplitude) can be positioned on the radar waveform with amplitude and time measurements displayed on the computer monitor. Utility programs, used in subsequent signal processing and necessary for measurement of the emitted radar waveform and noise cancellation, are contained in the calibration section.

The signal-processing software developed included modifications to existing software related to bridge deck testing. This software was written in C programming language, for high-speed, efficient execution. The additions to current software include the introduction of new

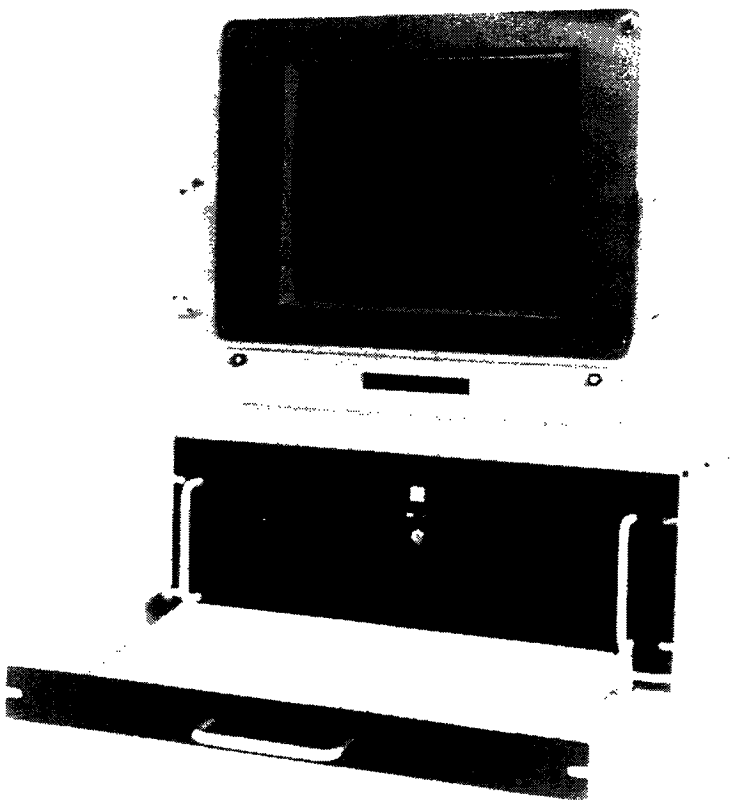

Figure 3-2. 80486 computer system developed for radar data acquisition/signal processing.

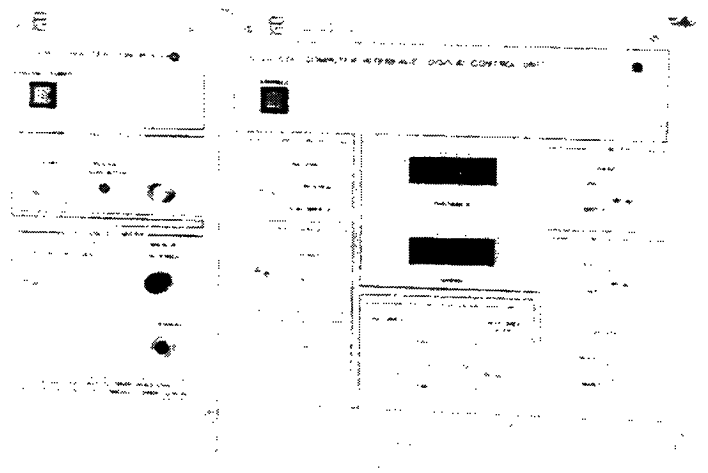

Figure 3-3. Rackmount CDU.

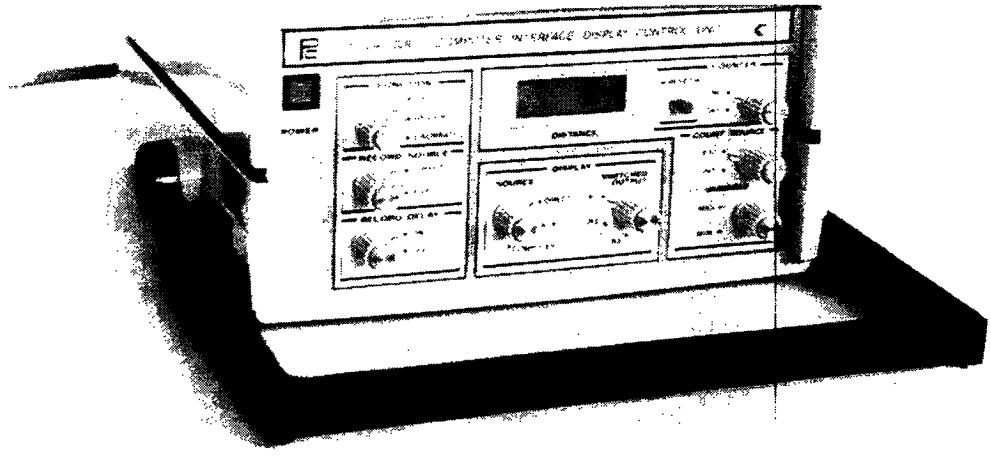

Figure 3-4. Portable CDU.

routines to implement the algorithms described in Chapter 6 relating to the attenuation (I/A) discriminant. The current radar-processing software utilizes both automated and user-assisted tracking algorithms for detection and identification of signals in the radar waveform, thus making the software easy to use by personnel who are unskilled in radar signal analysis. The software also allows user input of special parameters at user discretion, such as initial asphalt overlay thickness and initial cover thickness to top the reinforcing steel. This processing software uses the I/A threshold for delamination detection at top reinforcing steel and estimation of the repair area, described in Chapter 6. Another capability of this software is the measurement of the average depth of the top reinforcing steel. This depth measurement along with the detection and calculation of delamination area provides a means for estimation of concrete removal volumes.

4

Analytical Model

Introduction

To develop an understanding of radar propagation in an asphalt-covered bridge deck, a multi-layered, lossy (conductive) dielectric model was developed. After an understanding of the basic model was developed, the effects of reinforcing steel, moisture, and chloride were established. Finally, delaminated bridge deck concrete was modeled under both dry and wet conditions.

Bridge Deck Model

General

An asphalt-covered bridge deck pavement can be modeled as a lossy, four-layer dielectric. Assume that the first and last layer have infinite thickness. In this model, it is assumed that all materials are purely dielectric in nature and nonmagnetic, and that the radar radiates downward or normal to the pavement surface. The radio frequency energy generated by the radar first propagates from antenna to air. This emitted signal then encounters an air/asphalt boundary where, as stated earlier, a portion of the signal power traverses the dielectric boundary. The remaining power is reflected from the boundary in accordance with the relationship between transmitted and reflected energy at a dielectric boundary. This also describes the RF transmission and reflection at the A/C interface and at the deck bottom, i.e., at the concrete-to-air interface.

The layers of reinforcing steel also reflect energy. Metal objects effectively reflect all impinging RF energy. However, due to their small cross-sectional area relative to the antenna radiation pattern, only a very small portion of the energy is actually reflected back to the radar antenna.

Each material also causes the traversing signal to attenuate in part. Power loss can be accounted for using conventional electromagnetic theory for plane waves in lossy media (10). The power loss factor, a, for one-way propagation over a distance, D, is described in equation 4-1. For losses resulting from round trip propagation, D is replaced with $2D$.

$$a = e^{-2D(2\ pi\ f/c)\ [(e_r/2)[(1+\tan^2 g)0.5-1]]0.5} \tag{4-1}$$

where

f = frequency,
D = one-way path length in meters,
tan(g) = loss tangent, and
c = velocity of light.
e_r = relative dielectric constant (ratio of the dielectric constant of the medium to that of free space, e_r/e_o)

The loss tangent in equation 4-1 is defined as

$$\tan (g) = s/(2\ \pi\ fe_0e_r) \tag{4-2}$$

where

e_0 = 8.854×10^{-12} fd/m and
s = conductivity in the medium, mho/cm

Consider the diagram in Figure 4-1. showing the bridge deck cross section with associated radar ray diagram. The transmitted signal, with power, P_t, is shown impinging at normal

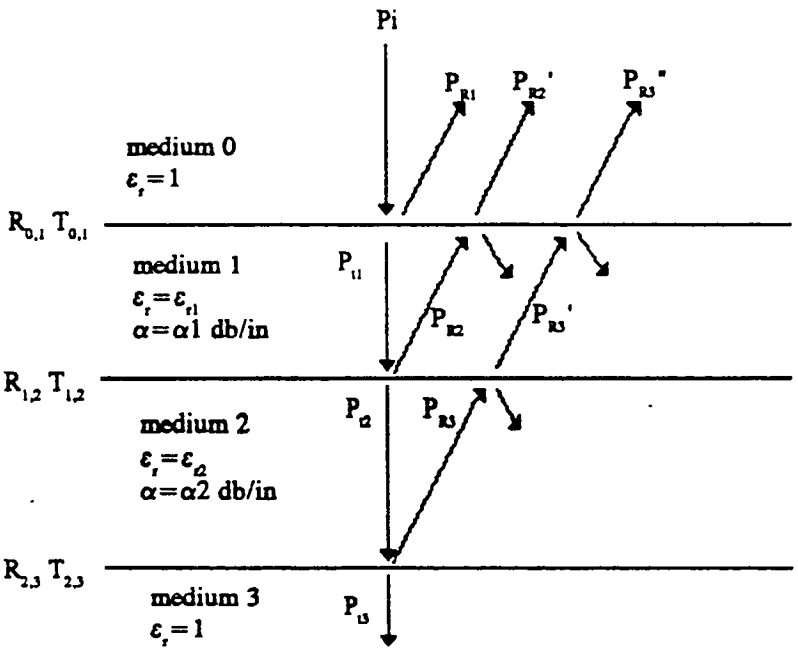

Figure 4-1. Bridge deck pavement modeled as four-layer dielectric.

incidence with the surface of the air to asphalt boundary, media 0 to 1. Power is reflected in accordance with the power reflection coefficient, $R_{0,1}$. From equation 4-3, the power observed at the antenna, Pr_1, corresponding to the reflection from the surface is given as:

$$P_{r1} = P_i (R_{0,1}) \tag{4-3}$$

P_{r1} and P_i are measured quantities from the radar waveform, and $R_{0,1}$ can be calculated from these measurements. Likewise, the transmitted power through the boundary is determined by the transmission coefficient, $T_{0,1} = 1\text{-}R_{0,1}$. The power actually coupled through the boundary

is $P_i(1-R_{0,1})$, or equivalently, $P_i(T_{0,1})$. In traversing medium 1, the signal experiences attenuation, a_1. At the A/C interface (media 1 to 2), the signal is reflected in accordance with the power reflection coefficient, $R_{1,2}$. Therefore, the power actually observed corresponding to the asphalt to concrete interface, P_{r2}', is then given as:

$$P_{r2}' = P_i\,(R_{1,2})\,[(T_{0,1})\,(a_1)]^2 \tag{4-4}$$

For medium 2, with relative dielectric e_{r3} and a power loss factor of (a_2), the power observed corresponding to the echo from the bottom of the bridge deck, P_{r3}'', at the antenna is:

$$P_{r3}'' = P_i(R_{2,3})\,[(T_{0,1})(a_1)(T_{1,2})(a_2)]^2 \tag{4-5}$$

The power reflection and transmission coefficients from medium n to medium $n+1$ can be solved, based on the following relationship:

$$R_{n,n+1} = [(e_{r\,n}{}^{0.5} - e_{r\,n+1}{}^{0.5}) / (e_{r\,n}{}^{0.5} + e_{r\,n+1}{}^{0.5})]^2 \tag{4-6}$$

where

$e_{r\,n}$ = relative dielectric constant of medium n and
$e_{r\,n+1}$ = relative dielectric constant of medium $n+1$.

This simplified model can be used as a basis for the calculation of the amplitude of reflected and transmitted signals at dielectric boundaries. However, it is only approximate, since the equations above do not take into account other factors, such as the scattering width of the dielectric boundaries, wavefront divergence (beam spreading), or the effective aperture area of the receiving antenna. These factors are not considered here.

Effect of Reinforcing Steel

The model to this point does not include the response from the embedded reinforcing steel in the concrete. The rebar layers can be modeled as a rectangular wire grid. We assume that the grid is completely embedded in a dielectric material (concrete) with a relative permittivity of 9 and that the material is lossless. The grid is constructed with bar spacing, d, in both directions, and bar diameter D_1 for longitudinal bars, and D_2 for transverse bars. The rebar diameter is much less than the rebar spacing. The angle of incidence (the angle with respect to the direction normal to the surface) is assumed to be 0 degrees. The radar center frequency is 1 GHz with a wavelength of about 1 ft (30 cm) in free space. In concrete with

a relative dielectric of 9 the effective wavelength is about 4 in. (10 cm). The model can be simplified considerably by the fact that the scattering from the transverse bars (orthogonal polarization) is much less than that from the longitudinal bars (parallel polarization). Therefore, it is reasonable to replace the grid network with a parallel bar model. The reflected energy is actually at a maximum for signal polarization where the electric vector of the incident wave is parallel to the bar. Further, it can be shown that the elimination of the transverse bars from the model will not significantly affect the outcome.

For this simplified model, the power reflection coefficient, *R*, of the reinforcing steel grid can be expressed in the form (*11*):

$$R = [1 + 4 (\cos a)^{0.5}[d/l [\ln(d/ \text{pi } D_1) + Fc]]^2]^{-1} \quad (4\text{-}7)$$

where

a = angle of incidence, assumed to be 0 for this analysis,
d = longitudinal bar spacing, assumed to be 8 in.(20 cm),
l = wavelength of the radar wave in a dielectric of 9 (concrete),
D_1 = diameter of the longitudinal reinforcing steel, assumed to be 5/8 in.(16 mm), and
Fc = correction factor related to conductor spacing which for our case is very small, approximately equal to 0.

Under the conditions described above, the power reflection coefficient, *R*, is -15.3 dB. The voltage reflection coefficient for this case is -0.17, which is low. Consider the case where the longitudinal rebar spacing is 12 in. (30 cm) and 0.5 in. (13 mm) in diameter. The power reflection coefficient would then be -21.8 dB, resulting in a lower voltage reflection coefficient of only -0.08.

It can be seen that the power reflection coefficient decreases as radar frequency increases (wavelength decreases), or as the bar spacing increases or the bar diameter decreases. It is interesting to note that *R* increases greatly at angles nearer grazing, i.e., approaching 90 degrees from normal incidence. Therefore, it is evident that the radar antenna should be operated at the normal incidence for maximum efficiency and minimal reflection from reinforcing steel. This analytical model for reinforcing steel agrees with experimental laboratory results.

Effect of Moisture and Chloride

Moisture and chloride are commonly found in concrete bridge decks. It is known that concrete in sound condition normally holds relatively little moisture (typically 4 to 5 percent by weight). However, permeable concrete can hold significantly larger amounts of moisture. Chloride ions created from the dissolution of deicing salts penetrate into the concrete by diffusion, and, while taking several years to reach the depth of the reinforcing steel, can create an environment suitable for corrosion of the embedded steel when they reach a critical threshold chloride content level. The quantitative effect of moisture and chloride on the model will be discussed.

Change in Signal Attenuation

The signal attenuation caused by water in concrete is not known and is difficult to accurately determine experimentally because of the inherent impermeability of concrete and the difficulty in carrying out such an experiment. An alternative experiment was designed, which attempted to ascertain this information by using sand in place of concrete because of their electrical similarity and the ease by which moisture can be added and distributed throughout the sample. It was found that moisture had a significant effect relative to signal attenuation.

Chloride ions in concrete change the conductivity of the concrete as well. Chloride present in even a low-concentration water solution creates an environment wherein the concrete is very conductive and tends to dissipate or attenuate the RF energy. It was found that chloride present in concrete without moisture, however, does not cause signal attenuation.

To obtain a better understanding of the effect of conductivity changes, an analysis was performed to quantitatively determine the effect of increased material conductivity on signal attenuation while varying dielectric constant and signal frequency.

Attenuation (dB/in.) in a medium, in this case assumed to be concrete, can be expressed by the equation:

$$\text{Atten (dB/in.)} = -0.001635\ D\ f\ [e_r((1+\tan^2 g)^{0.5} -1)]^{0.5} \qquad (4\text{-}8)$$

where

f = frequency in MHz.
e_r = relative dielectric constant,
$\tan g$ = loss tangent, per equation (4-2), and
D = one way distance in inches.

Attenuation versus conductivity was examined as a function of dielectric constant and frequency. Frequencies ranging from 1.0 GHz to 2.0 GHz, corresponding to the center frequencies of 1.0 ns, 0.8 ns, and 0.5 ns pulses, respectively, were used. Conductivity values from 0.05 to 25.0 m mho/in., approximately (0.02 m mho/cm to 10.0 m mho/cm), equivalent to resistivities of approximately 20,000 ohm-in. and 40 ohm-in., respectively (50,000 ohm-cm and 100 ohm-cm), were selected as the range of values likely to be found in bridge decks. Five dielectric constant values, 4, 6.25, 9, 15, and 81 were used, which, except for the last, are representative of the range of dielectric values of concrete in bridge decks. The results are summarized in Figure 4-2, showing only the results for dielectric constant values of 4 and 9 and frequencies of 1 and 2 GHz. It is evident that attenuation increases with conductivity. Also, for a given level of conductivity and a given frequency, the signal attenuation increases with decreasing dielectric values, which is to be expected. It is generally accepted that corrosion of reinforcing steel is highly likely when concrete resistivity is less than 5,000 ohm-cm. For 2,000 ohm-in. (5,000 ohm-cm) (conductivity of 0.5 m mho/in. (0.2 m mho/cm) and a relative dielectric constant of 15, the expected attenuation is approximately -0.1 dB/in. (-0.04 dB/cm). This appears to be slightly lower than what has been observed in radar field tests, but it is on the same order of magnitude.

As shown in Figure 4-2, the attenuation is frequency dependent for conductivity values greater than about 2.5 m mho/in. (1 m mho/cm), such that higher frequencies are attenuated more than lower frequencies. Also, notice that the rate of increase of attenuation for 1-GHz signals is less than for 2-GHz signals.

Change in Concrete Reflection Coefficient

The addition of moisture and chloride in concrete will affect the complex reflection coefficient since they directly affect the relative dielectric constant and conductivity. At 1-GHz frequency, however, the conductivity must be quite large in order to significantly affect the reflection coefficient. At very great conductivity levels (greater than 2.5 mho/in. (1 mho/cm)), the reflection coefficient increases. It can be shown that the complex reflection coefficient is not appreciably effected at the 1-GHz frequency range with concrete

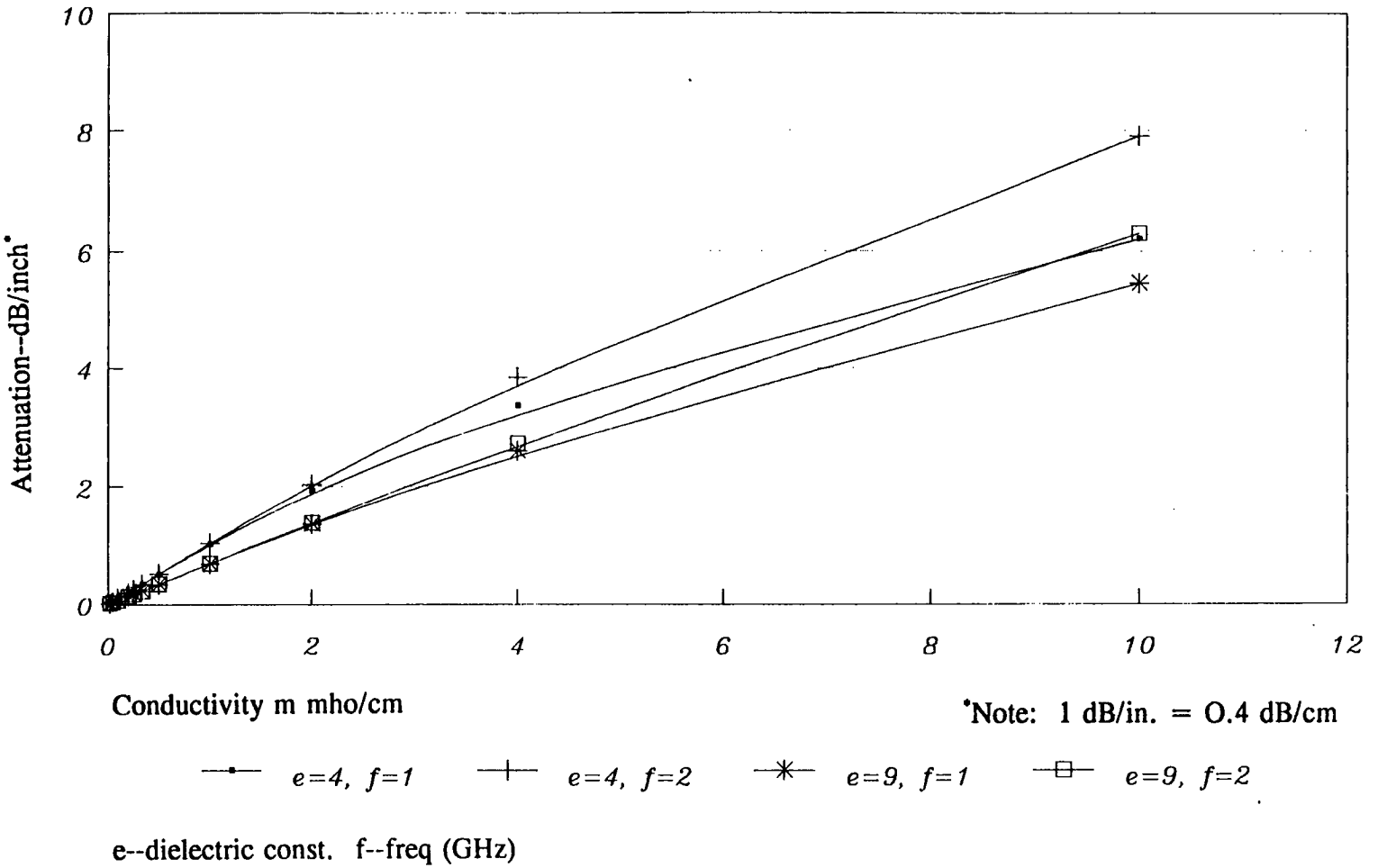

Figure 4-2. Attenuation versus conductivity for varying dielectric constant and frequency.

conductivity less than 0.25 mho/in. (0.1 mho/cm). For conditions encountered in the field, the concrete conductivity is always likely to be less than 0.1 mho/cm, and any changes in the reflection coefficient result primarily from relative dielectric changes. This means that chloride contents normally found in field concrete will not cause changes in the reflection coefficient and that changes are caused by moisture only. Experiments conducted, which varied chloride content up to 6 lb/yd^3 (3.6 kg/m^3), did not appreciably change the reflection coefficient.

Therefore, for a 1-GHz signal and typical conditions found in bridge decks, the voltage reflection coefficient can be adequately defined by the following simplified equation:

$$RHO_{n,n+1} = (e_{r\,n}^{0.5} - e_{r\,n+1}^{0.5}) / (e_{r\,n}^{0.5} + e_{r\,n+1}^{0.5}) \qquad (4\text{-}9)$$

where

$e_{r\,n}$ = relative dielectric constant of medium n and
$e_{r\,n+1}$ = relative dielectric constant of medium $n+1$.

The reflected signal only is observed in the radar return waveform from an interface. Therefore, all predictions of dielectric change must be made based on it. The reflection from the interface will increase when either of the following conditions are satisfied:

- The upper material relative dielectric, $e_{r\,n}$, decreases while at the same time the bottom material relative dielectric, $e_{r\,n+1}$, remains constant or increases; or

- The upper material relative dielectric, $e_{r\,n}$, remains constant and the lower material relative dielectric, $e_{r\,n+1}$, increases.

For the case at hand, moisture intrusion into concrete, the second condition will result. It can be seen from equation 4-9 that an increase in the dielectric constant $e_{r\,n+1}$ while $e_{r\,n}$ remains constant will result in a change in the echo reflected from the surface of the concrete, or an increase in the A/C interface echo.

Change in RF Propagation Velocity

Moisture intrusion into concrete causes an increase in the relative dielectric constant of the concrete. In addition to this increase in the reflection coefficient, the wavelength shortens and there is a reduction in the propagation velocity. The relative dielectric constant, e_r, is a

factor related to the dielectric of free space, e_0, (2.899×10^{-12} fd/f (8.854×10^{-12} fd/m)) and is always greater than or equal to unity. The propagation velocity in free space is equivalent to the speed of light, and for media with relative dielectric values greater than unity, the propagation velocity is decreased by the factor $(e_r)^{-0.5}$. The reduction in propagation velocity in a dielectric medium results in an increase in transit time through the medium. This is observed in the radar echo as a change in the time of occurrence of the signals making up the waveform. This can be shown as follows:

$$x = vt/2 \tag{4-10}$$

where

x = thickness of medium,
v = propagation velocity in medium, and
t = transit time through medium (two-way time).

The transit time can be measured from the radar echo and the propagation velocity can be expressed as follows:

$$v = c(e_r)^{-0.5} \tag{4-11}$$

where

c = speed of light, 9.8×10^8 f/sec (3×10^8 m/sec) and
e_r = relative dielectric constant of medium.

As the relative dielectric constant increases due to moisture intrusion into the concrete, the propagation velocity decreases. If the medium thickness does not change physically, the transit time or time separation between the echoes from the top and bottom of the medium must increase.

Experimental Verification

An experiment was designed to simulate the presence of water and chloride in concrete to determine the effect on an RF signal. In this experiment, it was possible to alter both the water content and the chloride, which are two elements that are commonly found in the bridge deck environment and are known to contribute to concrete deterioration in reinforced structures. The problem of introducing a variable, but well-defined, amount of water and

chloride to the medium was resolved by substituting sand for concrete, since the two materials are very similar from an electromagnetic standpoint.

The objectives of this experiment were twofold: first to measure the change in dielectric constant for different chloride and water concentrations, and second to determine the effect on signal attenuation when varying the dielectric of the sand-water mixture while maintaining constant chloride levels.

Five test forms were constructed with dimensions of 24 x 24 x 3.5 in. (61 x 61 x 9 cm) deep, containing 120 lb (55 kg) of dry sand each and a metal plate at the bottom, to reflect all of the RF energy. A 1-ns monocycle radar transmitter signal was directed normal to the surface.

To the first sample, only water was added in 1-percent by weight increments. The surface echo, bottom echo and transit time through the material were measured for each water concentration level. From this, the relative dielectric constant and attenuation of the mixture were calculated as described previously.

Chloride in precise, but varying, quantities was added to the remaining sand samples. Chloride concentrations of 0.30, 0.60, 1.2, and 6.0 lb/yd^3 (0.18, 0.36, 0.71, and 3.56 kg/m^3) were used for this experiment. Similar measurements of attenuation, reflection coefficient, and dielectric constant were made on each sample while varying the moisture content between 0 and 20 percent by weight. It is believed that this represents the moisture range that would typically be found in bridge deck concrete.

According to theory, the complex reflection coefficient is a function of both dielectric constant and conductivity in the medium. It is therefore necessary to find the change in reflection coefficient for the range of conductivity and dielectric normally encountered in bridge deck concrete. The measured reflection coefficient values for sand with different concentrations of water and chloride are shown in Figure 4-3. As expected, the reflection coefficient does vary with moisture content. However, there was very little change corresponding to variations of chloride content. It can be seen that for concentrations of water typically found in concrete, the reflection coefficient and relative dielectric constant do not deviate much with respect to the chloride amount. It is therefore concluded that typical amounts of chloride found in bridge deck concrete, 0 to 6 lb/yd^3 (0 to 3.6 kg/m^3), are insufficient to cause changes in the A/C reflection coefficient. This shows that reflection coefficient and dielectric changes in bridge deck concrete are not the result of chloride intrusion, but rather entrapped moisture, for chloride concentrations within this range. This supports the previous assumptions.

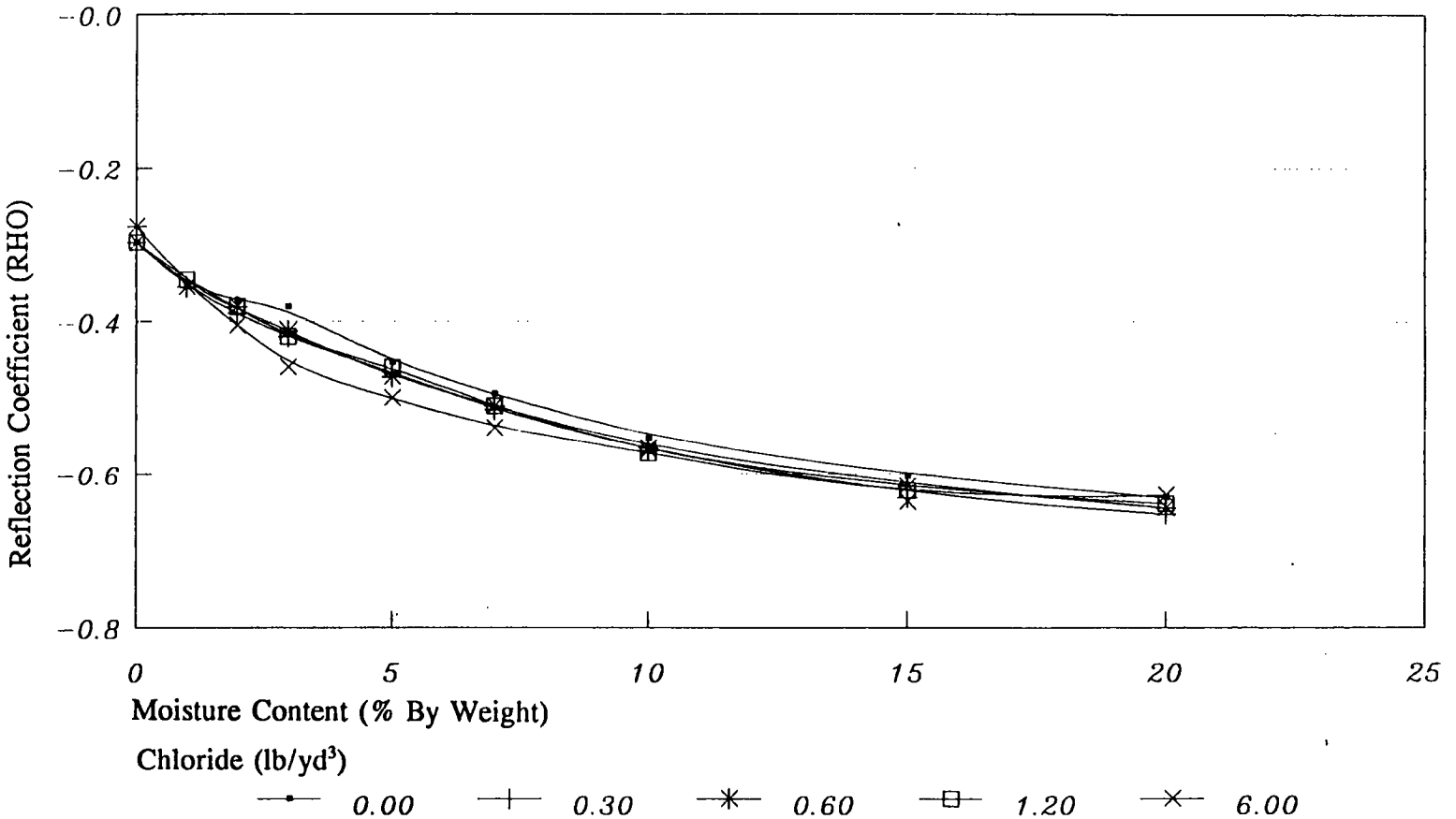

Figure 4-3. Reflection coefficient versus moisture content for varying chloride levels.

For bridge decks, two factors will affect attenuation in concrete: chloride and moisture. It was found in experiments using water-chloride solutions that attenuation increases with chloride content and with moisture content. This is illustrated in the set of curves shown in Figure 4-4. Although these curves were derived for sand, it is expected that those for concrete would likely be quite similar. In applying these curves to concrete, the range of expected signal attenuation can be determined based on chloride content for any given moisture concentration in the concrete. For example, if it is known that the concrete moisture content in delaminated concrete is 5 percent, then the signal attenuation would range from -0.4 to -3.0 dB/in. (-0.15 to -1.18 dB/cm) in the delaminated concrete, depending on chloride content. If the chloride content is also known, then the expected increase in signal attenuation can be estimated. For instance, a moisture concentration of 5 percent and a chloride content of 3 lb/yd^3 (1.8 kg/m^3) would yield an expected increase in signal attenuation of roughly -1.8 dB/in. (-0.71 dB/cm), over the depth of the delaminated concrete.

This type of relationship could also be used to locate concrete with a particular chloride concentration. However, the moisture content of the concrete must be known beforehand. Since the moisture in a material affects the dielectric constant of the material, a simple radar measurement of the dielectric constant will yield the moisture content, assuming a relationship is known between dielectric constant and moisture. This relationship can be obtained by way of experiment. Figure 4-5 shows the dielectric constant versus moisture content in sand. Although this curve may not be identical to that of concrete, it should be fairly close if a relative dielectric y-intercept value of 6.25 for dry concrete is used. Therefore, with a radar measurement of the dielectric constant of concrete the moisture content can be estimated by using the extrapolated (upper) curve for concrete in Figure 4-5. Since the change in reflection coefficient and relative dielectric constant are essentially independent of chloride content (for the chloride concentrations expected in the field), any variations in chloride will not substantially affect this measurement. Once the concrete moisture is known, then the proper attenuation-chloride curve in Figure 4-4 can be used to predict the expected attenuation. Based on these results, it may be possible to determine locations on a bridge deck where a particular average chloride content exists, solely from radar measurements of dielectric and attenuation increase.

For example, suppose that it is desired to delineate the concrete having chloride contents greater than 3 lb/yd^3 (1.8 kg/m^3). Assume that the nominal attenuation of sound concrete is negligible when no chloride is present. A relative dielectric constant measurement of 12 is obtained for the concrete, resulting in a moisture content of about 7 percent (from the curve in Figure 4-5). Referring to Figure 4-4 and using the 7 percent moisture curve, the expected

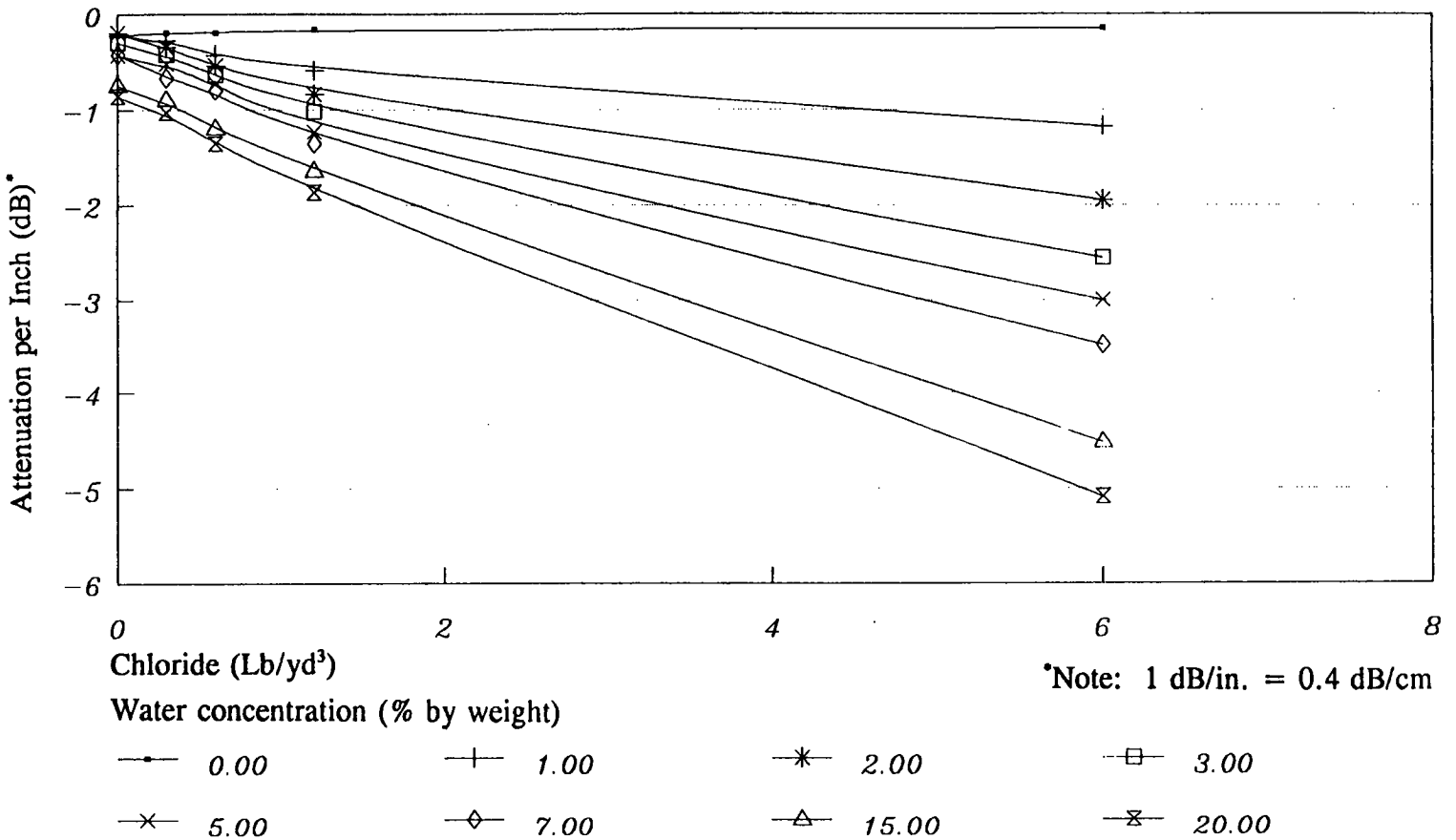

Figure 4-4. Attenuation versus chloride content for varying moisture contents.

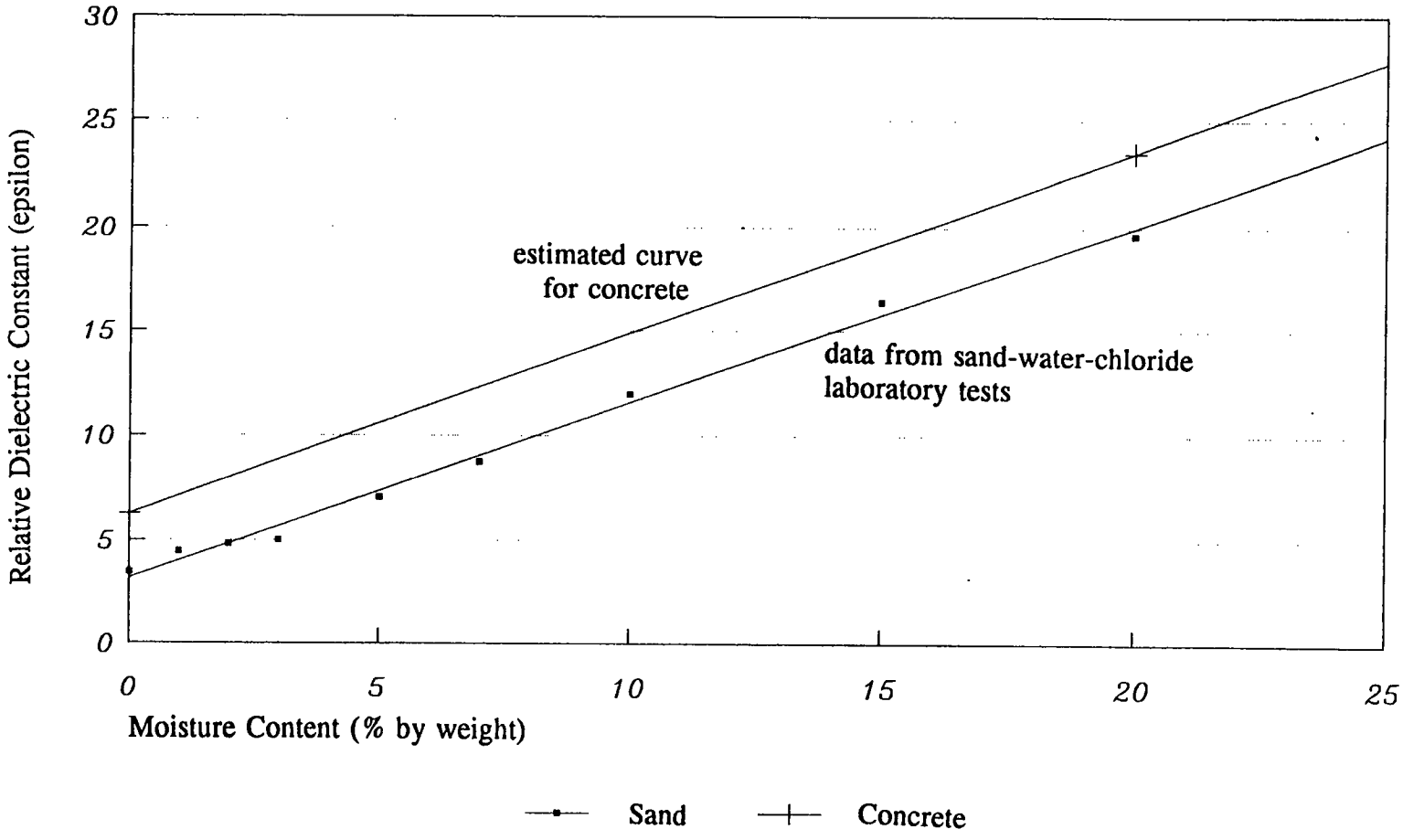

Figure 4-5. Relative dielectric constant versus moisture content.

increase in unit signal attenuation will be about -2.2 dB/in. (-0.87 dB/cm). The total increase in attenuation is the unit attenuation multiplied by the depth that the chloride has penetrated into the concrete.

According to this experiment, the approximate signal attenuation caused by moisture and chloride that will be experienced by a 1-ns radar signal will fall within the range of values shown in Table 4-1 for moisture concentrations between 1 percent and 20 percent by weight.

Table 4-1. Additional signal attenuation at 1 GHz caused by chloride as related to minimum and maximum moisture quantities in concrete.

Chloride Content (lb/yd^3)	Attenuation, dB/in	
	Minimum	Maximum
1	-0.5	-1.8
2	-0.7	-2.4
3	-0.8	-3.2
4	-0.9	-3.8
5	-1.1	-4.4
6	-1.2	-5.1

Note: 1 dB/in. = 0.4 dB/cm (approximately).
1 lb/yd^3 = 0.59 kg/m^3.

Computer Waveform Model

A model and algorithm were developed based on the superposition technique of time domain signals in accordance with their signal amplitude and phase, time delay, and attenuation in the media (12,13). This technique requires a prior knowledge of the magnitude of the emitted signal, number of media, relative dielectric constant for each of the media, and signal loss (specifically, the attenuation factor) in each media. It assumes normal wave incidence and nonmagnetic materials.

The amplitude of resulting reflections and re-reflections from a five-dielectric layer pavement are calculated along with their phase and corresponding time delay. Summing each of the reflections in relation to their time of occurrence yields a composite waveform corresponding to the media designated.

Software was developed for waveform generation based on this model. The software called WAVE, originally developed by Penetradar Corporation for different applications, was modified and run on an 80486-based PC.

The program WAVE accepts input from the user relative to the number of media, the dielectric constant of each media, the attenuation of each material, and the thickness of each layer. Reflections of the original emitted signal, occurring at each dielectric interface, are summed in a 1 x V(t) array. A radar waveform is then constructed based on the input parameters and the superposition of the reflections. The resultant waveforms are then displayed on the computer monitor or printed in hardcopy. This program is used later in analysis of field data (Chapter 6) and in comparison with actual radar waveforms to determine the makeup of various deck pavements and the dielectric, and attenuative properties and thicknesses of deck pavement layers.

Delamination Modeling

General

Subsequent to the development of an accurate RF model for delamination in concrete, the causes of delamination must be defined. Delamination is the result of steel corrosion caused by moisture and dissolved deicing salts entering into the concrete to the depth of reinforcing steel and creating an environment whereby corrosion can occur.

In one case, chlorides can diffuse through concrete at a rate dependent on the permeability of the concrete, eventually working down to the level of the top reinforcing steel. This usually requires many years and results in concrete with very high chloride levels. Depending on the permeability of the concrete, it may contain high amounts of moisture as well. In another case, cracking of the concrete surface can act as a means for passage of chloride and water to the reinforcing steel. The critical form of cracking here is "settlement" cracking, which may occur during construction parallel to and directly above the reinforcing steel. Its occurrence is a function of reinforcement cover. This can occur in sound concrete that has low permeability to moisture. In this case, the concrete above a delamination may not contain significant amounts of chloride or moisture.

It was previously shown that RF propagation is sensitive to changes in material conductivity. From the experiments conducted and the discussion in previous sections, it was determined that chloride ions from deicing salt cause an increase in the overall conductivity of the medium when introduced into a material with water present. It was further determined that RF attenuation increases with an increase in conductivity. However, the dissolved salt (chloride) in the absence of moisture does not significantly affect the conductivity or signal attenuation. Also, in the instance where delamination occurs from moisture and chloride passage through surface cracks to the reinforcing steel, the concrete may not possess high moisture levels or exhibit high signal attenuation.

Therefore, two situations exist with respect to delaminated concrete, which are based on the presence of moisture in the delaminated concrete. When moisture is present, the delamination can be determined by signal attenuation resulting from conductivity increase caused by the water/chloride solution in the concrete.

When the delaminated concrete is relatively dry, the delamination could be caused by either chloride and moisture passage through cracks in the concrete or by permeable concrete, which at the time is dry. In either of these instances, the attenuative effects caused by the combination of chloride and water will not be present and the delamination can be detected directly.

Delamination Model for Dry Concrete

Consider the case where the concrete is dry. It is desirable to determine, analytically, if a delamination is detectable and then compute the reflection coefficient at the concrete to air gap while varying the gap size. The following assumptions are made: the incident radar wave is normal to the surface of the media and to the delamination plane, and the materials

are nonmagnetic. For simplicity, the bridge deck will be modeled as a three-layer dielectric with the first and third layers as infinite in thickness, but with the same relative dielectric constant. The delamination will be considered as a planar gap of varying thickness, as shown in Figure 4-6. We want to determine *R* the complex reflection coefficient, at the 1-2 boundary as computed in medium 1. Using conventional transmission line theory, we can determine the intrinsic impedance of each of the materials as:

$$N_n = N_0 \left[(e_{r\,n})^{0.5}(1+S_n{}^2/w{}^2 e_0{}^2 e_{r\,n}{}^2)^{0.25}\right]^{-1}\left[e^{j0.5\tan^{-1}(s_n/we_0e_{r\,n})}\right] \quad (4\text{-}12)$$

where

N_0 = 377 ohm,
$e_{r\,n}$ = relative dielectric constant of media *n*,
e_0 = 8.854 x 10^{-12},
s_n = conductivity of *n*th medium, assumed to be zero in the lossless case, and
w = $2(\pi) f$, where f = frequency

The propagation factors *a* and *b* can be calculated as follows:

$$(al)_n = (wd/c)\left[(e_{r\,n}/2)((1+ (S_n/we_0e_{r\,n})^2)^{0.5} - 1)\right]^{0.5} \quad (4\text{-}13)$$

$$(bl)_n = (wd/c)\left[(e_{r\,n}/2)((1+ (S_n/we_0e_{r\,n})^2)^{0.5} + 1)\right]^{0.5} \quad (4\text{-}14)$$

Using the transmission line equation, the impedance of layer 2 can be found:

$$Z_2 = N_2\left[Z_3 + N_2 \tanh((al)_2 + j(Bl)_2)\right] / \left[N_2 + Z_3 \tanh((al)_2 + j(Bl)_2)\right] \quad (4\text{-}15)$$

where

Z_2 = impedance at the upper interface of medium 2,
Z_3 = load impedance on medium 2, and
N, *al*, *bl* are defined by equations 4-12, 4-13, and 4-14.

The desired complex reflection coefficient, *R*, at the upper interface between mediums 1 and 2 is computed using:

$$R = (Z_2 - N_1)/(Z_2 + N_1) \quad (4\text{-}16)$$

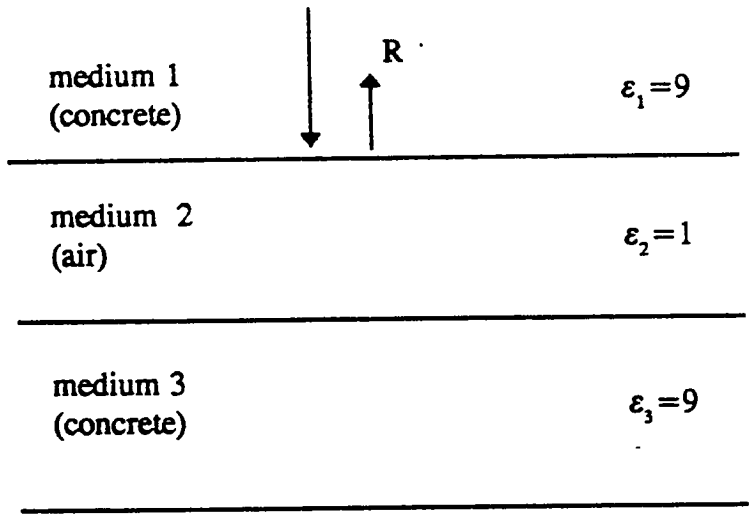

Figure 4-6. Reflection from planar gap between lossless media.

The complex reflection coefficient at the concrete/delamination gap can be computed with the assumptions that $e_{r1} = e_{r3} = 9$ and $e_{r2} = 1$. Conductivity, s, for the lossless case is zero. Several commutations of R were made while varying medium 2-layer thickness and at two frequencies, 1 GHz and 2 GHz. The power reflection coefficient varies with frequency and gap size in accordance with Figure 4-7. As expected, the power reflection coefficient approaches zero as the gap size approaches zero since $e_{r1} = e_{r3}$. The reflection coefficient for a 1-GHz applied signal, is about -28 dB (rho = 0.04) for a 0.05-in. (1.25-mm) delamination. This reflection coefficient would likely produce a echo smaller than, but on the same order of magnitude as, the other internal echoes (such as the reinforcing steel). This suggests that a 0.05-in. (.127-cm) concrete delamination should theoretically be detectable under the conditions described.

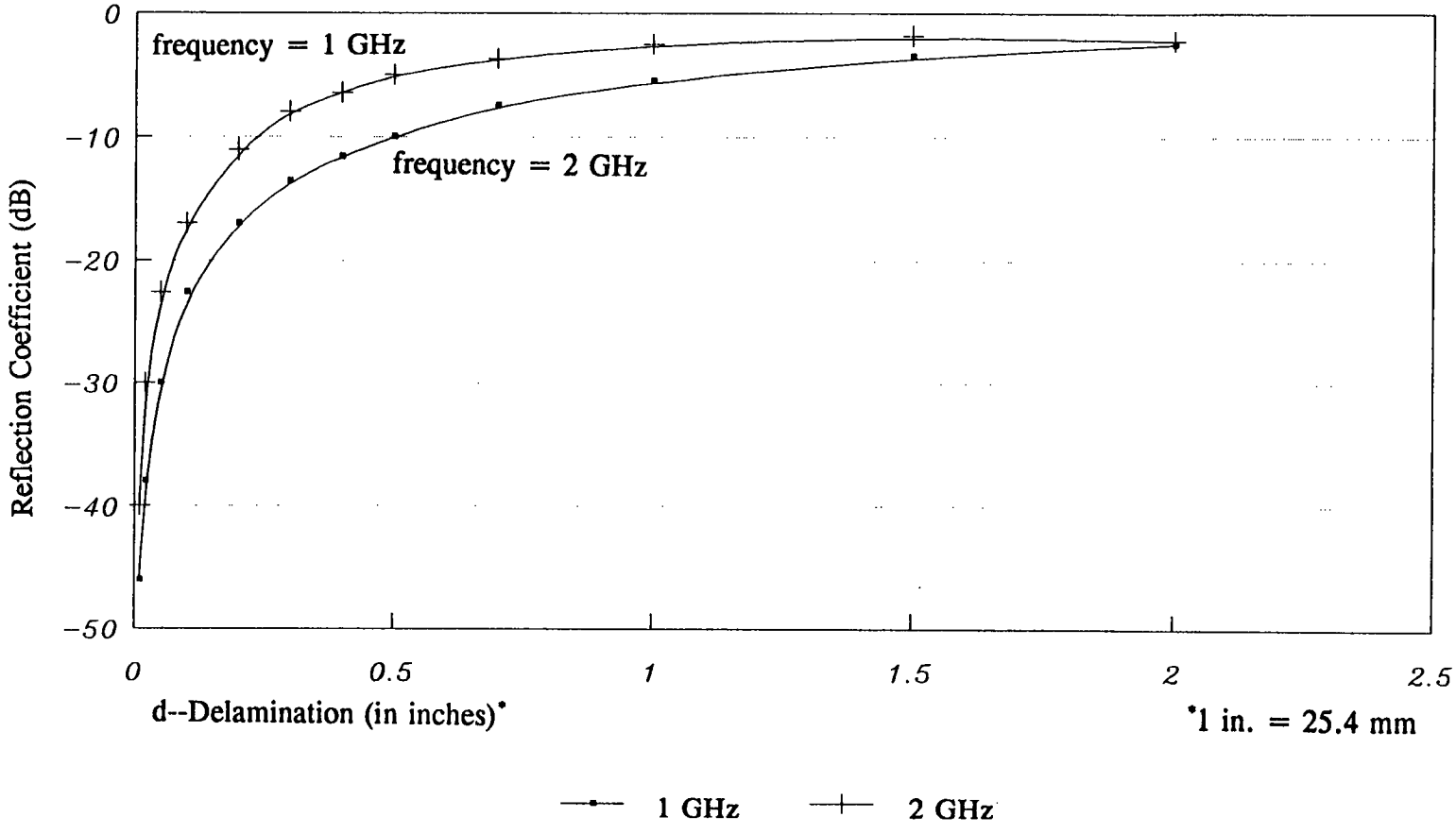

Figure 4-7. Power reflection coefficient versus delamination gap size at two frequencies.

Comparison of the 1-GHz and 2-GHz curves shows the reflection coefficient to be strongly dependent on frequency. Consequently, a higher frequency signal produces a larger reflection coefficient, which implies that higher frequency will yield better detectability of small air gaps or delaminations, in the lossless case. For example, a 0.1-in. (.25-cm) air gap produces a -23-dB reflection coefficient at 1 GHz, whereas at 2 GHz, the reflection coefficient is approximately 6 dB greater (-17 dB). Theoretically, for dry concrete, it is preferable to utilize a transmitted signal with the widest bandwidth possible but, only in a medium with very low loss.

It is concluded that a laminar air gap caused by a delamination in dry concrete can be detected. However, detectability decreases with decreasing gap size and the ability to detect thin laminar air gaps increases with frequency.

Delamination Model for Concrete with Moisture

When conductivity and relative dielectric in the concrete medium are high, such as in the case of high moisture and high chloride content, waveform analysis techniques are less effective because of the attenuative effects suffered by the radar signal, primarily in the region where chloride concentration is greatest, i.e., 1 to 2 in. (2.5 to 5 cm) from the surface. Initially, this would appear to be a problem. However, this attenuative effect can be used to detect delamination and quantify the delaminated area.

It has been shown that the occurrence of moisture and chloride together in concrete in large quantities creates a condition where signal attenuation, high signal reflection at the surface of the concrete, and decrease in propagation velocity of the radar signal take place. All these conditions have been found to be related to the occurrence of delamination in varying degrees. However, two of these conditions, high signal reflectivity and decrease in propagation velocity are dependent only on the moisture contained in the concrete (for typical bridge deck concrete). While moisture does contribute to the development of delamination, it is unlikely that delamination would occur without chloride present. Since the two discriminants are not responsive to chloride in concrete, it may be possible to have a false indication of delamination by detecting high moisture accumulation at the concrete surface or in a water-soaked waterproofing membrane. At best, the increase in reflectivity and decrease in propagation velocity, effects on the RF signal are indicators of moisture presence in concrete and can only be loosely connected with the occurrence of delamination.

In contrast, signal attenuation is related to both moisture and chloride and is responsive to both when they occur together. Aside from direct detection of a delamination, which is

possible only during dry concrete conditions, the most reasonable of the three radar discriminants is signal attenuation. Theoretically, this should best define the presence of delamination, since it is the only discriminant that is actually responsive to the changes in conductivity caused by chloride in concrete. This is not to say that moisture intrusion into concrete cannot serve as an delamination indicator, since permeable concrete in poor condition will often absorb considerable amounts of moisture and chloride. Rather, moisture absorption as given by changes in the dielectric constant of concrete (resulting in increases in reflectivity in concrete and propagation velocity decrease) simply provides an indication of the permeability of the concrete rather than the direct tendency for delamination.

Therefore, it is concluded that delamination in concrete with high moisture levels can be detected by measurement of the radar signal attenuation in response to the elements causing delamination, i.e., moisture and chloride.

In the case of moisture, assume that the delaminated concrete contains a uniform amount of chloride. If a_0 is the nominal attenuation in sound concrete with minimal moisture and chloride, and a_1 is the attenuation in the deck with the addition of moisture and chloride, then the additional signal attenuation, a_d, that results when a delamination is present is simply the difference between attenuation a_1 and attenuation a_0.

This can be described analytically using the attenuation equation, with relative dielectric and conductivity as variables. For example, using equation 4-8, the attenuation a_0 and a_1 at 1 GHz can be calculated. Although exact values for relative dielectric and conductivity cannot be easily ascertained, typical values are used. For the calculation of a_1, assume that the relative dielectric constant in permeable concrete with high chloride is 16; this value is typical of wet concrete. Also assume that the average conductivity in the deck in this case is 2.5 m mho/in. (1.0 m mho/cm) (resistivity = 400 ohm-in. (1,000 ohm-cm)), i.e., well within the range of conductivity reported to cause delamination. From equation 4-8 the signal attenuation is approximately -0.5 dB/in. (-0.2 dB/cm) For the calculation of a_0, assume that the relative dielectric constant is 9 and the conductivity is 0.13 m mho/in. (0.05 m mho/cm) (resistivity = 8,000 ohm-in. (20,000 ohm-cm)). Here the signal attenuation is about -0.035 dB/in. (-0.014 dB/cm). Therefore, the additional attenuation resulting from the increased conductivity caused by moisture and chloride in the concrete is -0.465 dB/in. (0.186 dB/cm) using these values. For the entire bridge deck, say 8 in. (20.32 cm) in thickness, the total increase in attenuation would be -7.44 dB.

A comparison can be made between this attenuation value and chloride quantity, indicated by the attenuation versus chloride curves in Figure 4-4, to determine whether this attenuation level does actually correspond to an amount of chloride known to cause delamination. Since

the moisture and chloride are likely to be concentrated in the top portions of the concrete, the attenuation will not be uniformly distributed throughout. Rather, it will be greatest in the top portion of the concrete. If the total increase in attenuation of -7.44 dB occurs in the top 2-in. (5.08-cm) layer, then the unit attenuation is 1.86 dB/in. (0.744 dB/cm). Referring to Figure 4-4, this attenuation level corresponds to roughly 1.5 lb/yd^3 (0.9 kg/m^3) for wet concrete conditions (15-percent moisture), or about 3 lb/yd^3 (1.8 kg/m^3) for a more typical 5-percent moisture content. Although approximate values were used for this analysis, the chloride quantity results are not unreasonable, since delamination is known to occur in this range of chloride concentrations.

5

Field Data Acquisition

Radar Data and Test Sites

During the course of the project, a total of 22 bridge decks were examined with radar in order to ascertain the validity of delamination discriminants (Chapter 6) and to develop a means for estimation of bridge deck delamination. The bridge deck tests were conducted using GPR equipment installed on a van and configured as shown in Figure 5-1. Figure 5-2 shows radar testing in progress. The test procedure that was observed involved the gathering of radar data in longitudinal scan passes along the lengths of the bridge decks. The scan passes were spaced either 18 or 24 in. (46 or 61 cm) apart in the transverse direction so that the majority of the deck area would be covered. The antenna looked downward with an effective elliptical "footprint" of about 9-in. (23 cm) longitudinal by 16 in. (41 cm) in the transverse direction. These dimensions, however, will vary with antenna height. Locational accuracy was established by means of a precision distance-marker wheel that was attached to the van. Much of the radar data gathered during the project was recorded on conventional magnetic tape. Later in the project, the developed data acquisition equipment (Chapter 3) was used for direct digitization of acquired waveforms.

Bridges were selected for testing from three states (New York, Virginia, and Vermont), representing a range of severe to moderate climates. Field tests were conducted in varying

Figure 5-1. Vehicular-installed radar systems used for bridge decks tests.

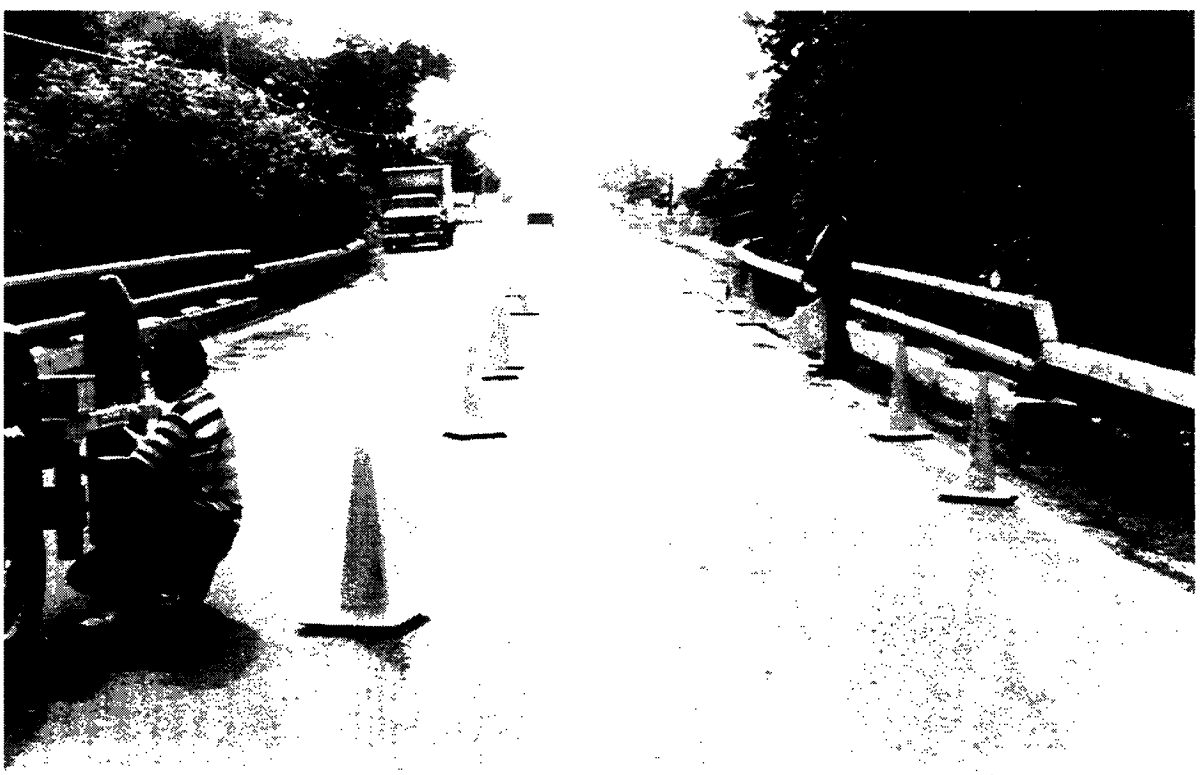

Figure 5-2. Radar testing in progress.

climatic conditions and under various moisture conditions. Two test sites were re-examined under different moisture conditions in order to observe the variation in radar signal relative to moisture change and the ability to detect delamination. The list of bridges tested is presented in Table 5-1.

Ground Truth Data

Ground truth data were collected to determine correlations between potential radar delamination discriminants and actual bridge deck delamination. This ground truth data consisted of core samples, chain drag soundings, and actual repair quantities after reconstruction, when possible. Core samples and actual repair quantities were the preferred ground truth methods used for the determination of the delamination threshold. However, chain drag soundings were used as well when the former were unavailable. Ground truth testing in progress on one of the bridge decks is shown in Figure 5-3.

It should be emphasized that each of the ground truth methods has an accuracy and false alarm rate associated with it, and that no method is without error. It was found in several cases that there was considerable discrepancy between different ground truth methods. For example, in some cases areas were designated as delaminated by chain drag, but failed to show high negative half-cell potential measurements. Obviously, if the reinforcement had corroded to the point of producing delaminations, high corrosion potentials should have been observed. In one instance, the bridge on Route 211 over the Shenandoah River in Virginia, there was a very large difference between chain drag sounding predictions and actual repair quantities.

Table 5-1. Bridges tested.

Bridge	Location	Date
2804	Route 1--Bristol, VA	Dec. 7, 1988
2805	Route 1--Bristol, VA	Dec. 7, 1988
1011	Mount Jackson, VA	Dec. 8, 1988
1019	Route 211--Shenandoah River, VA	Dec. 8, 1988
1029	Route 1--Shinning Creek, VA	March 14, 1988
1088	Route 58--Perrins Creek, VA	March 15, 1989
6125	Route 810--White Hall, VA	March 16, 1989
	I-91--SB Williams River, Rockingham, VT	July 17, 1989
1024420	Route 39--Walnut Creek, Forestville, NY	May 21, 1989
1030120	Route 77--Eighteen Mile Creek, NY	June 19, 1989
1034710	Route 93--Twelve Mile Creek, NY	June 19, 1989
1034710	Route 93--Twelve Mile Creek, NY	Aug. 2, 1989
	I-87--Major Deegan Expressway, NYC	Aug. 17, 1989
62640	Route 62 over Route 17E--Kennedy, NY	March 2, 1990
62650	Route 62 over Route 17W--Kennedy, NY	March 2, 1990
950DX	Over I-90 East--Ripley, NY	April 23, 1990
950DX	Over I-90 West--Ripley, NY	April 23, 1990
62640	Route 62 over Route 17E--Kennedy, NY	April 24, 1990
	Route 60 over I-90--Dunkirk, NY	April 24, 1990
	Route 1 South--Meherin River, VA	Aug. 15, 1990
	Route 1 South--Nottoway Creek, VA	Aug. 15, 1990
	Route 220--Blackwater River, VA	Aug. 15, 1990

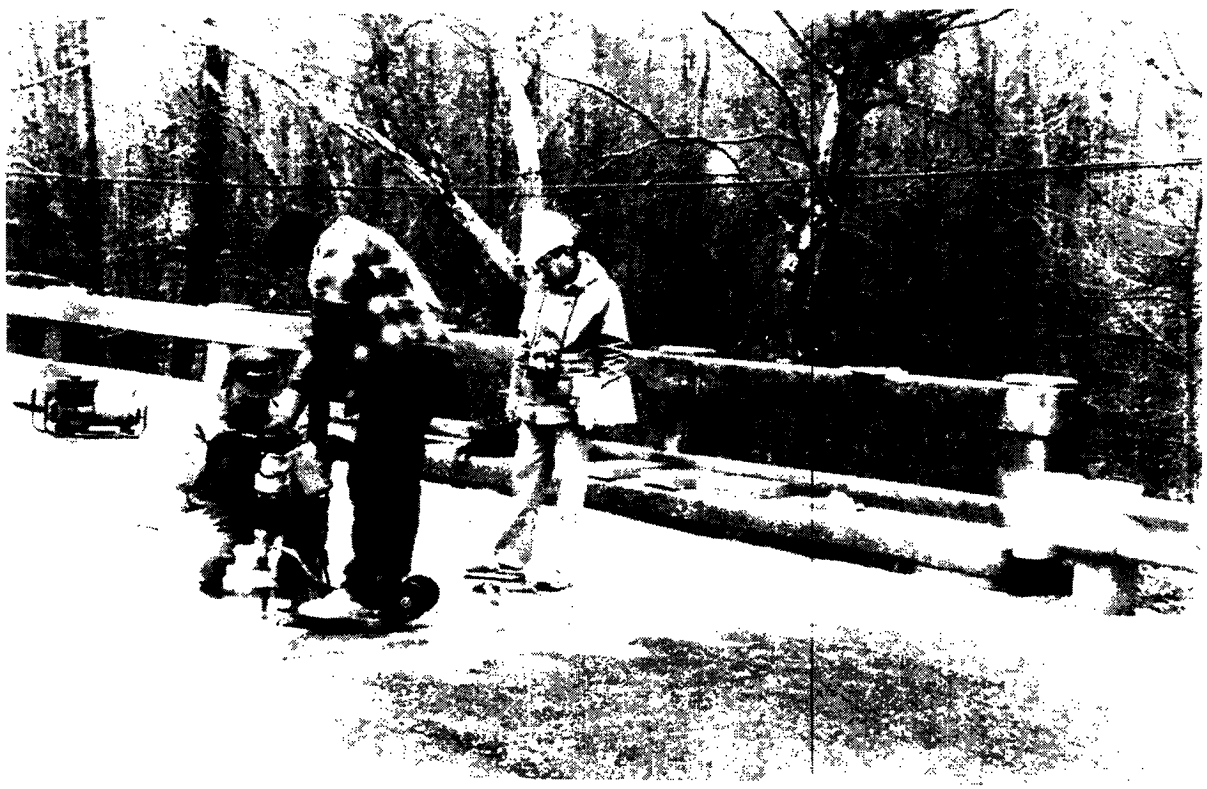

Figure 5-3. Ground truth testing in progress on one of the test bridge decks.

6

Development of Delamination Discriminants

Analysis and Evaluation of Radar Field Data

An extensive field test program was conducted from December 1988 through August 1990 on 22 bridge decks (see Chapter 5). Radar data were gathered from each deck along with visual information and photographs relating to the top and bottom surface conditions. Ground truth data also were obtained consisting of core samples, data from manual sounding of the concrete (chain drag), half-cell electrical potential measurements, and chloride ion content. When possible, actual repair locations and quantities were also compared with radar results.

In accordance with the objectives, it was desired to ascertain the deterioration discriminant that provides the optimal prediction of delamination location and simultaneously yields the best prediction of the actual quantity of delamination. To achieve this, the radar waveforms were examined in detail. Since the radar produces data at very high data rates, 50 range sweeps or waveforms per second, several thousand waveforms were gathered for each bridge deck under examination. Raw radar data were stored primarily on magnetic tape and visually examined for unusual conditions or anomalies. These anomalies were categorized as follows:

- Change in reflectivity from deck surface (*S*);
- Increase in reflectivity from asphalt to concrete (A/C);
- Increase or decrease in echo from reinforcing steel (I/R), (D/R);

- Signal distortion (W);
- Decrease in propagation velocity through the bridge deck (P/V); and
- Increase in signal attenuation (I/A).

These anomalous waveform conditions were quantified using semiautomatic computer detection techniques and by manual detection when the computer methods were not possible. Radar waveforms were analyzed using specialized hardware and software for radar-signal processing developed previously by Penetradar Corporation. These provided an analysis capability for measurement of amplitude and phase of radar signals, signal averaging, and thresholding of signals based on fixed values or variables related to the signal mean value. This equipment employed electronic gates to isolate particular signals in the waveform. The analyst selected a portion of the waveform to be digitized, after which it was input to a microcomputer where statistical analysis was performed and examination of the subject discriminant was made. The computer used as inputs the radar waveform (after proper preprocessing and gating), the radar synchronization trigger, and the wheel pulse signal corresponding to distance. The radar data rate was substantially decreased by digitizing radar data upon occurrence of a radar trigger pulse, but only after the distance count from the marker wheel had changed. In this manner, one radar scan was digitized every 3 in. (7.62 cm) instead of at a 50-Hz rate.

Previously developed signal processing software was used for measurement of signal amplitude and statistical processing based on threshold values. The threshold values were either fixed or variable as determined by the analyst, and the processing program made detections based on the threshold value. The "fixed threshold" simply used a predefined voltage value, which was directly compared with each signal, whereas the "variable threshold" developed a value based on a user-defined fraction of the mean value of the signal, averaged over a predetermined distance, typically 100 ft (30.5 m). For deterioration discriminants where this equipment was not effective, such as those requiring signature analysis, a simple manual detection process was utilized. An analyst monitored the radar signal and performed the detection manually by "flagging" the computer with a pushbutton connected to an I/O port upon observation of the desired signal anomaly. In either case, the processed data were stored in computer memory as a 1 x (MN) array where M is the length of the bridge deck in feet and N is the number of radar inspection passes. So that radar detections could be compared with ground truth data, the 1 x (MN) array was then mapped into an N x M array. This could then be printed in hard copy format by a computer mapping program used for generating plan view representations of the bridge deck showing the location of the previously stored detections.

The approach undertaken for determination of the optimal delamination discriminant was simple but very labor-intensive. Mappings were produced for each of the indicators and compared with ground truth data for locational accuracy. At that point, a qualitative decision was made for each indicator's success in detecting delamination based on correspondence and overlap of radar indicator detections and ground truth data (specifically chain drag or actual repair quantity). For illustration, selected mappings from sections of two bridge decks, the Route 211 bridge over the Shenandoah River in Luray, Virginia, and the I-91 South bridge over Williams River in Rockingham, Vermont, are shown overlaid with ground truth maps in Figures 6-1 through 6-4. Special software was written such that ground truth data can be manually entered into the computer in a 1 x (*MN*) array similar to that for the radar discriminants so that the radar detection map and ground truth map can be superimposed.

Two forms of ground truth data were gathered from the Route 211 bridge deck in Virginia: chain drag and actual repair quantity. The radar test was performed first with the asphalt overlay present. Afterwards, the asphalt was removed and a chain drag survey was conducted. Delaminated concrete removal was then performed subsequent to the chain drag soundings. The repairs were initially based on the chain drag predicted locations, but were later extended to areas where additional delaminated concrete was found. The plots in Figure 6-1 give the intersection of radar data (which has been compared to a fixed attenuation threshold) and actual repaired areas. The (+) designation shows the radar attenuation discriminant, and the (o) designation shows the actual repaired areas. A combination of the two indicate the case where both radar and ground truth are in agreement. The (+) marking alone indicates an overestimation, and the (o) marking shows an underestimation. Examination of this mapping shows that there is a definite correlation between an increase in RF attenuation (I/A) and delamination, as per the repaired areas. For the entire bridge deck and the selected attenuation threshold, the radar detected all but one of the major delaminated areas, resulting in an overall true detection rate of 0.702, an underestimation figure of 0.298, and an overestimation figure of 0.419. Obviously, these figures can be adjusted to maximize detection or minimize underestimation and overestimation by adjustment of the attenuation threshold, depending on the objective. In this case, the results from the radar test using the attenuation discriminant at the selected threshold value produced better predictions of the true detection rate and underestimation rate than the usually reliable chain drag. The chain drag true detection figure was 0.567, the underestimation figure was 0.433, and the overestimation figure was 0.221. All of the figures represent area ratios.

Radar tests were conducted on the I-91 Rockingham Bridge and a chain drag survey performed subsequent to asphalt removal.

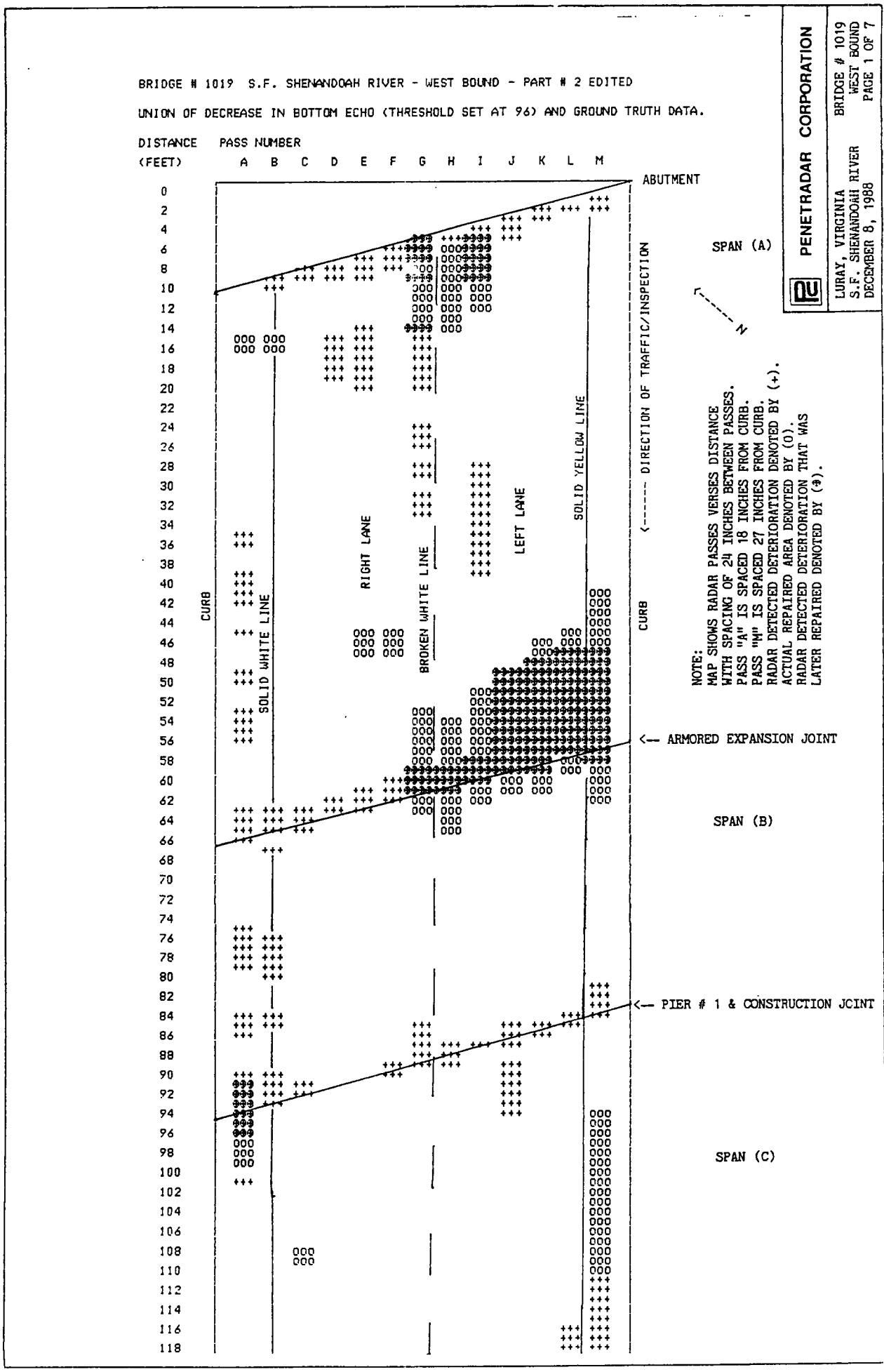

Figure 6-1. Radar (attenuation of signal) and ground truth data for a part of the Route 211 bridge over the Shenandoah River in Luray, Virginia.

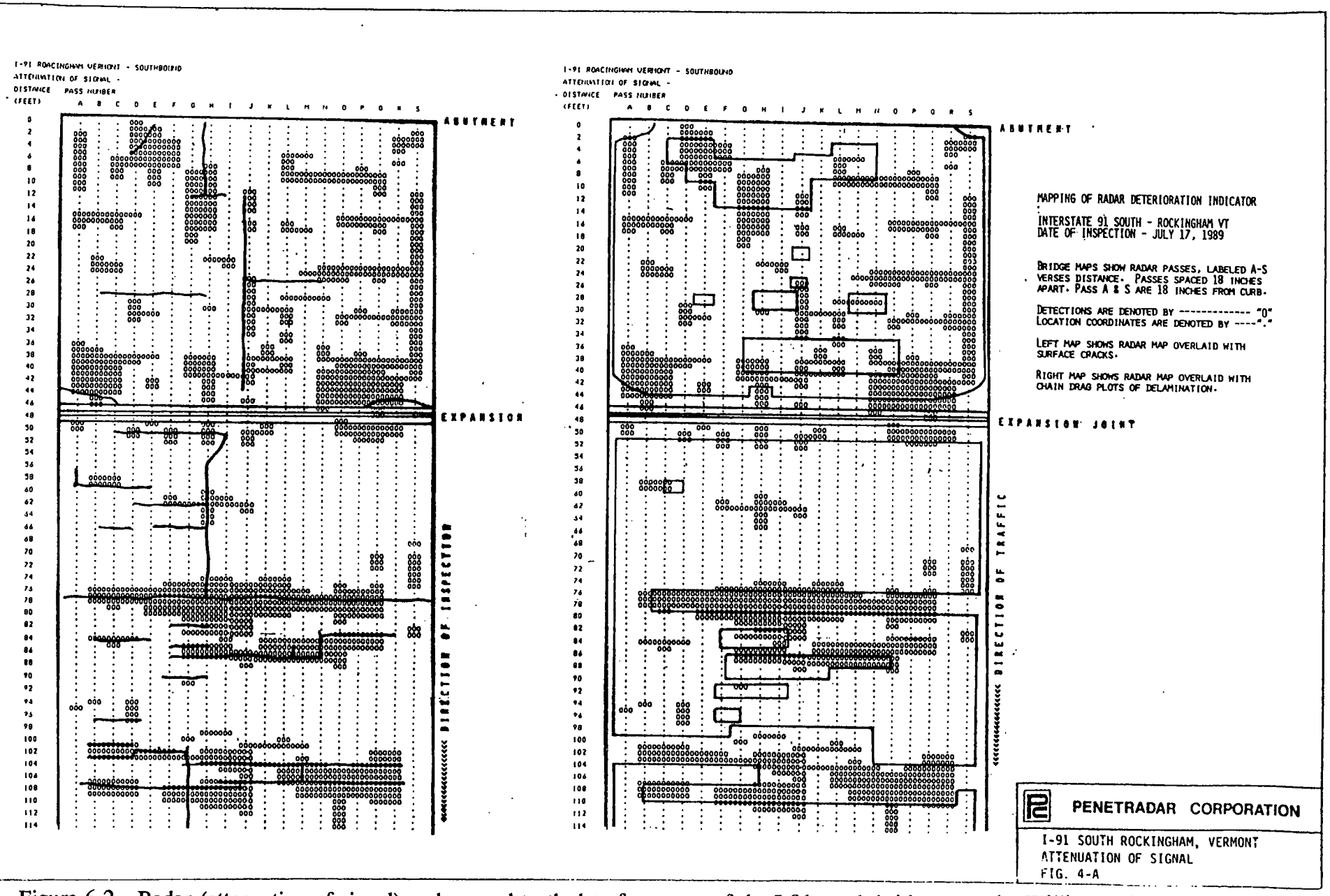

Figure 6-2. Radar (attenuation of signal) and ground truth data for a part of the I-91 south bridge over the Williams River in Rockingham, Vermont.

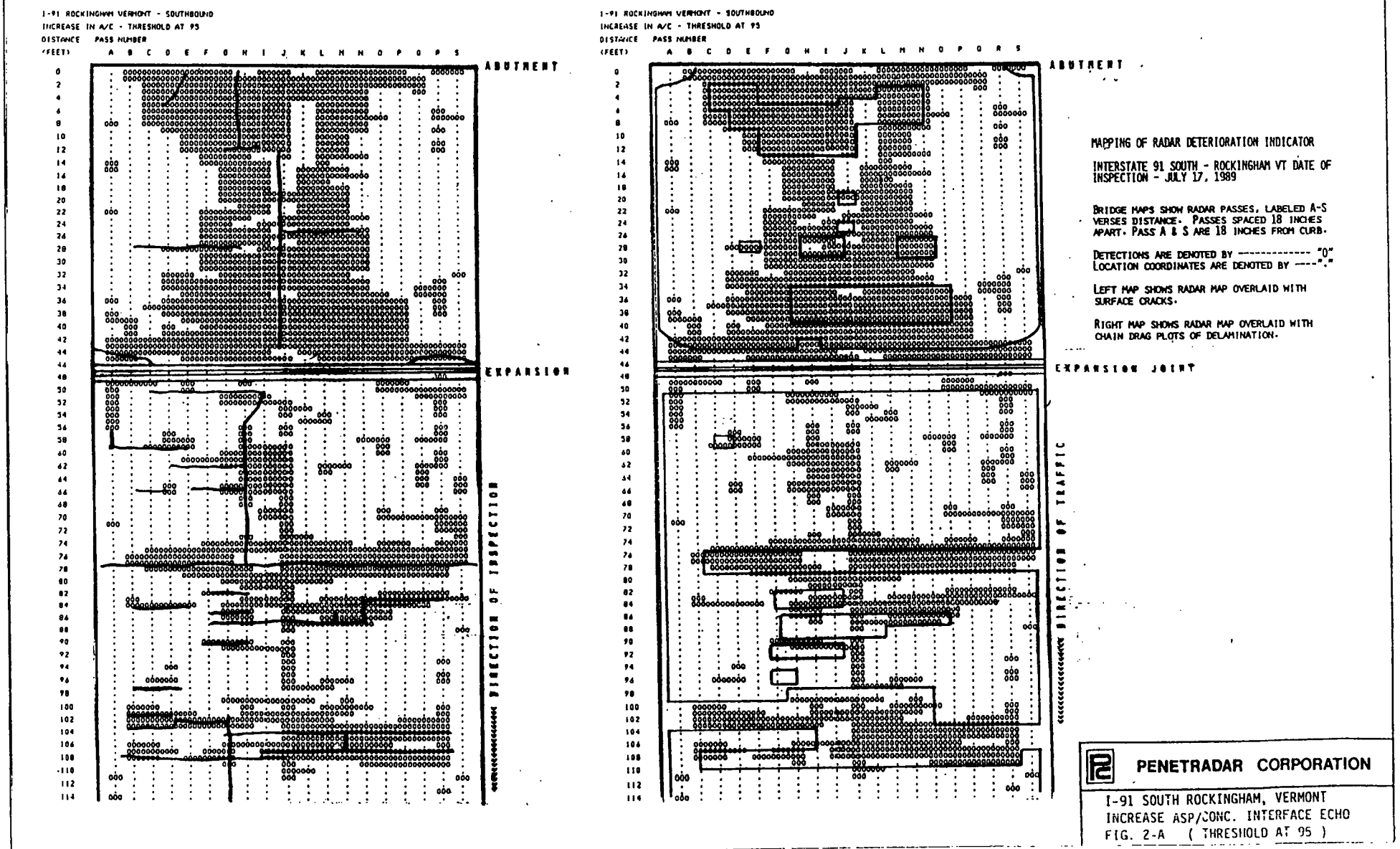

Figure 6-3. Radar (increase in asphalt/concrete interface echo) and ground truth data for a part of the I-91 south bridge over the Williams River in Rockingham, Vermont.

Figure 6-4. Radar (decrease in propagation velocity) and ground truth data for a portion of the I-91 south bridge over the Williams River in Rockingham, Vermont.

Locations of chain drag detected delaminations were logged and plotted as were locations of vertical cracks in the concrete, for correlation with radar data. The left map in Figure 6-2 depicts the radar attenuation discriminant (shown "O" symbols) with surface cracks superimposed. The right map shows chain drag soundings (shown as outlined areas) superimposed on radar data. Again, there was found to be a definite correspondence between the radar attenuation discriminant and chain drag detected delamination. In some areas, it appeared that the attenuation discriminant was also responsive to the vertical cracks in the concrete. Figures 6-3 and 6-4 show similar mappings for the increase in A/C reflectivity and decrease in P/V discriminants.

An alternative method for determination of the optimal deterioration indicator was employed for bridge decks where core samples were taken. Since it was impossible to obtain sufficient numbers of core samples to adequately outline an actual delaminated area, a spreadsheet program was written to calculate the correlation between radar indicator and actual incidence of deterioration. A detailed analysis of radar indicators for one tested bridge deck, the Route 1 bridge deck over Shinning Creek in Virginia, is shown in Figures 6-5 through 6-8. Although we are interested primarily in concrete delamination, several types of deterioration are listed. Each possible discriminant is shown in terms of its detection and false alarm rate for detecting both affected and nonaffected areas. The results of the study of deterioration indicators for this bridge deck are typical of most of the decks where this analysis was performed and tend to support the delamination models previously discussed.

Comparison of Radar Delamination Discriminants

Change in Reflectivity from Deck Surface

The energy reflected from the asphalt surface, referred to as the surface echo, was measured in some bridge decks. It was found that the surface echo did change from one deck to another, and from one location on a deck to another. However, little correlation was found to exist between these areas of change and actual deteriorated areas. Changes in surface echo amplitude were likely caused by changes in moisture in the asphalt, but had little to say about the concrete itself. No additional investigation was conducted with this discriminant.

Increase in Reflectivity from Asphalt to Concrete

The RF energy reflected from the A/C interface was measured quantitatively. Both fixed and variable thresholds were used in processing. Increases in this signal were compared to

RADAR VS CORE STATISTIC WORKSHEET
DATE: 01-Mar-90
TIME: 09:35:36 AM
BRIDGE: SHINNING CREEK
RADAR INDICATOR: ATTENUATION OF SIGNAL
ANALYST: K.J.S.

1) OVERALL CORRELATION FOR EACH TYPE OF DETERIORATION.

TYPE OF PERCENTAGE	TOP DELAM	BOTTOM DELAM	TOP SCALING	ASPHALT DETER.	BOTTOM SCALING	TOP BAR CORROS.	BOT.BAR CORROS.	SALT STAINS	SURFACE CRACK	HIGH CHLORIDE
A) DETECTION IN RADAR ONLY (NY)	20.00%	24.00%	32.00%	40.00%	20.00%	32.00%	12.00%	32.00%	24.00%	40.00%
B) DETECTION IN CORE ONLY (YN)	12.00%	28.00%	0.00%	8.00%	0.00%	16.00%	20.00%	0.00%	8.00%	0.00%
C) DETECTED IN BOTH (YY)	20.00%	16.00%	8.00%	0.00%	20.00%	8.00%	28.00%	8.00%	16.00%	0.00%
D) AREA OF NO DETECTIONS (NN)	48.00%	32.00%	60.00%	52.00%	60.00%	44.00%	40.00%	60.00%	52.00%	60.00%
TOTALS:	100.00%	100.00%	100.00%	100.00%	100.00%	100.00%	100.00%	100.00%	100.00%	100.00%

STATISTICS PER TYPE OF DETERIORATION	TOP DELAM	BOTTOM DELAM	TOP SCALING	ASPHALT DETER.	BOTTOM SCALING	TOP BAR CORROS.	BOT.BAR CORROS.	SALT STAINS	SURFACE CRACK	HIGH CHLORIDE
1) PROBABILITY OF DETECTING AFFECTED AREA	62.50%	36.36%	100.00%	0.00%	100.00%	33.33%	58.33%	100.00%	66.67%	ERR
2) PROBABILITY OF DETECTING NON-AFFECTED AREA	70.59%	57.14%	65.22%	56.52%	75.00%	57.89%	76.92%	65.22%	68.42%	60.00%
3) FALSE ALARM RATE OF DETECTING AFFECTED AREA	29.41%	42.86%	34.78%	43.48%	25.00%	42.11%	23.08%	34.78%	31.58%	40.00%
4) FALSE ALARM RATE OF DETECTING NON-AFFECTED AREA	37.50%	63.64%	0.00%	100.00%	0.00%	66.67%	41.67%	0.00%	33.33%	ERR
OVERALL CORRELATION RATE:	68.00%	48.00%	68.00%	52.00%	80.00%	52.00%	68.00%	68.00%	68.00%	60.00%

2) UNION AND INTERSECTION CORRELATION FOR SELECTED TYPES OF DETERIORATION.

DETERIORATION CHARACTERISTICS USED ARE: TOP SCALING - BOTTOM SCALING - SALT STAINS ON BOTTOM OF DECK

STATISTICS PER TYPE OF DETERIORATION	UNION	INTERSECTION	TYPE OF PERCENTAGE	UNION	INTERSECTION
1) PROBABILITY OF DETECTING AFFECTED AREA	100.00%	ERR	A) DETECTION IN RADAR ONLY (NY)	12.00%	40.00%
2) PROBABILITY OF DETECTING NON-AFFECTED AREA	83.33%	60.00%	B) DETECTION IN CORE ONLY (YN)	0.00%	0.00%
3) FALSE ALARM RATE OF DETECTING AFFECTED AREA	16.67%	40.00%	C) DETECTED IN BOTH (YY)	28.00%	0.00%
4) FALSE ALARM RATE OF DETECTING NON-AFFECTED AREA	0.00%	ERR	D) AREA OF NO DETECTIONS (NN)	60.00%	60.00%
OVERALL CORRELATION RATE:	88.00%	60.00%	TOTALS:	100.00%	100.00%

FORMULAS USED FOR COMPUTING RESPECTIVE STATISTICS

1) C/(B+C)
2) D/(1-(B+C))
3) A/(1-(B+C))
4) B/(B+C)

Figure 6-5. Evaluation of signal attenuation as a discriminant for various indicators of deterioration--Shinning Creek bridge, Virginia.

RADAR VS CORE STATISTIC WORKSHEET — DATE: 01-Mar-90, TIME: 09:40:50 AM — BRIDGE: SHINNING CREEK, RADAR INDICATOR: INCREASE IN A/C ECHO, ANALYST: K.J.S.

1) OVERALL CORRELATION FOR EACH TYPE OF DETERIORATION.

TYPE OF PERCENTAGE	TOP DELAM	BOTTOM DELAM	TOP SCALING	ASPHALT DETER.	BOTTOM SCALING	TOP BAR CORROS.	BOT.BAR CORROS.	SALT STAINS	SURFACE CRACK	HIGH CHLORIDE
A) DETECTION BY RADAR ONLY (NY)	20.00%	24.00%	32.00%	40.00%	20.00%	32.00%	16.00%	32.00%	24.00%	40.00%
B) DETECTION IN CORE ONLY (YN)	12.00%	28.00%	0.00%	8.00%	0.00%	16.00%	24.00%	0.00%	8.00%	0.00%
C) DETECTED IN BOTH (YY)	20.00%	16.00%	8.00%	0.00%	20.00%	8.00%	24.00%	8.00%	16.00%	0.00%
D) AREA OF NO DETECTIONS (NN)	48.00%	32.00%	60.00%	52.00%	60.00%	44.00%	36.00%	60.00%	52.00%	60.00%
TOTALS:	100.00%	100.00%	100.00%	100.00%	100.00%	100.00%	100.00%	100.00%	100.00%	100.00%

STATISTICS PER TYPE OF DETERIORATION	TOP DELAM	BOTTOM DELAM	TOP SCALING	ASPHALT DETER.	BOTTOM SCALING	TOP BAR CORROS.	BOT.BAR CORROS.	SALT STAINS	SURFACE CRACK	HIGH CHLORIDE
1) PROBABILITY OF DETECTING AFFECTED AREA	62.50%	36.36%	100.00%	0.00%	100.00%	33.33%	50.00%	100.00%	66.67%	ERR
2) PROBABILITY OF DETECTING NON-AFFECTED AREA	70.59%	57.14%	65.22%	56.52%	75.00%	57.89%	69.23%	65.22%	68.42%	60.00%
3) FALSE ALARM RATE OF DETECTING AFFECTED AREA	29.41%	42.86%	34.78%	43.48%	25.00%	42.11%	30.77%	34.78%	31.58%	40.00%
4) FALSE ALARM RATE OF DETECTING NON-AFFECTED AREA	37.50%	63.64%	0.00%	100.00%	0.00%	66.67%	50.00%	0.00%	33.33%	ERR
OVERALL CORRELATION RATE:	68.00%	48.00%	68.00%	52.00%	80.00%	52.00%	60.00%	68.00%	68.00%	60.00%

2) UNION AND INTERSECTION CORRELATION FOR SELECTED TYPES OF DETERIORATION.

DETERIORATION CHARACTERISTICS USED ARE: TOP SCALING - BOTTOM SCALING - SALT STAINS ON BOTTOM OF DECK.

STATISTICS PER TYPE OF DETERIORATION	UNION	INTERSECTION	TYPE OF PERCENTAGE	UNION	INTERSECTION
1) PROBABILITY OF DETECTING AFFECTED AREA	100.00%	ERR	A) DETECTION IN RADAR ONLY (NY)	12.00%	40.00%
2) PROBABILITY OF DETECTING NON-AFFECTED AREA	83.33%	60.00%	B) DETECTION IN CORE ONLY (YN)	0.00%	0.00%
3) FALSE ALARM RATE OF DETECTING AFFECTED AREA	16.67%	40.00%	C) DETECTED IN BOTH (YY)	28.00%	0.00%
4) FALSE ALARM RATE OF DETECTING NON-AFFECTED AREA	0.00%	ERR	D) AREA OF NO DETECTIONS (NN)	60.00%	60.00%
OVERALL CORRELATION RATE:	88.00%	60.00%	TOTALS:	100.00%	100.00%

FORMULAS USED FOR COMPUTING RESPECTIVE STATISTICS

1) C/(B+C)
2) D/(1-(B+C))
3) A/(1-(B+C))
4) B/(B+C)

Figure 6-6. Evaluation of increase in asphalt/concrete interface echo as a discriminant for various indicators of deterioration--Shinning Creek bridge, Virginia.

RADAR VS CORE
STATISTIC WORKSHEET

DATE: 01-Mar-90
TIME: 09:21:18 AM

BRIDGE: SHINNING CREEK
RADAR INDICATOR: INCREASE IN REBAR ECHO - TOP MAT
ANALYST: K.J.S.

1) OVERALL CORRELATION FOR EACH TYPE OF DETERIORATION.

TYPE OF PERCENTAGE	TOP DELAM	BOTTOM DELAM	TOP SCALING	ASPHALT DETER.	BOTTOM SCALING	TOP BAR CORROS.	BOT.BAR CORROS.	SALT STAINS	SURFACE CRACK	HIGH CHLORIDE
A) DETECTION IN RADAR ONLY (NY)	16.00%	12.00%	24.00%	24.00%	24.00%	24.00%	24.00%	24.00%	20.00%	24.00%
B) DETECTION IN CORE ONLY (YN)	24.00%	32.00%	8.00%	8.00%	20.00%	24.00%	48.00%	8.00%	20.00%	0.00%
C) DETECTED IN BOTH (YY)	8.00%	12.00%	0.00%	0.00%	0.00%	0.00%	0.00%	0.00%	4.00%	0.00%
D) AREA OF NO DETECTIONS (NN)	52.00%	44.00%	68.00%	68.00%	56.00%	52.00%	28.00%	68.00%	56.00%	76.00%
TOTALS:	100.00%	100.00%	100.00%	100.00%	100.00%	100.00%	100.00%	100.00%	100.00%	100.00%

STATISTICS PER TYPE OF DETERIORATION	TOP DELAM	BOTTOM DELAM	TOP SCALING	ASPHALT DETER.	BOTTOM SCALING	TOP BAR CORROS.	BOT.BAR CORROS.	SALT STAINS	SURFACE CRACK	HIGH CHLORIDE
1) PROBABILITY OF DETECTING AFFECTED AREA	25.00%	27.27%	0.00%	0.00%	0.00%	0.00%	0.00%	0.00%	16.67%	ERR
2) PROBABILITY OF DETECTING NON-AFFECTED AREA	76.47%	78.57%	73.91%	73.91%	70.00%	68.42%	53.85%	73.91%	73.68%	76.00%
3) FALSE ALARM RATE OF DETECTING AFFECTED AREA	23.53%	21.43%	26.09%	26.09%	30.00%	31.58%	46.15%	26.09%	26.32%	24.00%
4) FALSE ALARM RATE OF DETECTING NON-AFFECTED AREA	75.00%	72.73%	100.00%	100.00%	100.00%	100.00%	100.00%	100.00%	83.33%	ERR
OVERALL CORRELATION RATE:	60.00%	56.00%	68.00%	68.00%	56.00%	52.00%	28.00%	68.00%	60.00%	76.00%

2) UNION AND INTERSECTION CORRELATION FOR SELECTED TYPES OF DETERIORATION.

DETERIORATION CHARACTERISTICS USED ARE: TOP DELAMINATIONS - BOTTOM DELAMINATIONS

STATISTICS PER TYPE OF DETERIORATION	UNION	INTERSECTION
1) PROBABILITY OF DETECTING AFFECTED AREA	26.67%	25.00%
2) PROBABILITY OF DETECTING NON-AFFECTED AREA	80.00%	76.19%
3) FALSE ALARM RATE OF DETECTING AFFECTED AREA	20.00%	23.81%
4) FALSE ALARM RATE OF DETECTING NON-AFFECTED AREA	73.33%	75.00%
OVERALL CORRELATION RATE:	48.00%	68.00%

TYPE OF PERCENTAGE	UNION	INTERSECTION
A) DETECTION IN RADAR ONLY (NY)	8.00%	20.00%
B) DETECTION IN CORE ONLY (YN)	44.00%	12.00%
C) DETECTED IN BOTH (YY)	16.00%	4.00%
D) AREA OF NO DETECTIONS (NN)	32.00%	64.00%
TOTALS:	100.00%	100.00%

FORMULAS USED FOR COMPUTING RESPECTIVE STATISTICS

1) C/(B+C)
2) D/(1-(B+C))
3) A/(1-(B+C))
4) B/(B+C)

Figure 6-7. Evaluation of increase in top mat rebar echo as a discriminant for various indicators of deterioration--Shinning Creek bridge, Virginia.

RADAR VS CORE STATISTIC WORKSHEET
DATE: 01-Mar-90
TIME: 09:27:47 AM
BRIDGE: SHINNING CREEK
RADAR INDICATOR: DISTORTED REBAR ECHO - TOP MAT.
ANALYST: K.J.S.

1) OVERALL CORRELATION FOR EACH TYPE OF DETERIORATION.

TYPE OF PERCENTAGE	TOP DELAM	BOTTOM DELAM	TOP SCALING	ASPHALT DETER.	BOTTOM SCALING	TOP BAR CORROS.	BOT.BAR CORROS.	SALT STAINS	SURFACE CRACK	HIGH CHLORIDE
A) DETECTION IN RADAR ONLY (NY)	28.00%	24.00%	36.00%	32.00%	32.00%	28.00%	16.00%	28.00%	28.00%	36.00%
B) DETECTION IN CORE ONLY (YN)	24.00%	32.00%	8.00%	4.00%	16.00%	16.00%	28.00%	0.00%	16.00%	0.00%
C) DETECTED IN BOTH (YY)	8.00%	12.00%	0.00%	4.00%	4.00%	8.00%	20.00%	8.00%	8.00%	0.00%
D) AREA OF NO DETECTIONS (NN)	40.00%	32.00%	56.00%	60.00%	48.00%	48.00%	36.00%	64.00%	48.00%	64.00%
TOTALS:	100.00%	100.00%	100.00%	100.00%	100.00%	100.00%	100.00%	100.00%	100.00%	100.00%

STATISTICS PER TYPE OF DETERIORATION	TOP DELAM	BOTTOM DELAM	TOP SCALING	ASPHALT DETER.	BOTTOM SCALING	TOP BAR CORROS.	BOT.BAR CORROS.	SALT STAINS	SURFACE CRACK	HIGH CHLORIDE
1) PROBABILITY OF DETECTING AFFECTED AREA	25.00%	27.27%	0.00%	50.00%	20.00%	33.33%	41.67%	100.00%	33.33%	ERR
2) PROBABILITY OF DETECTING NON-AFFECTED AREA	58.82%	57.14%	60.87%	65.22%	60.00%	63.16%	69.23%	69.57%	63.16%	64.00%
3) FALSE ALARM RATE OF DETECTING AFFECTED AREA	41.18%	42.86%	39.13%	34.78%	40.00%	36.84%	30.77%	30.43%	36.84%	36.00%
4) FALSE ALARM RATE OF DETECTING NON-AFFECTED AREA	75.00%	72.73%	100.00%	50.00%	80.00%	66.67%	58.33%	0.00%	66.67%	ERR
OVERALL CORRELATION RATE:	48.00%	44.00%	56.00%	64.00%	52.00%	56.00%	56.00%	72.00%	56.00%	64.00%

2) UNION AND INTERSECTION CORRELATION FOR SELECTED TYPES OF DETERIORATION.

DETERIORATION CHARACTERISTICS USED ARE: BOTTOM REBAR CORROSION - SALT STAINS ON BOTTOM OF DECK.

STATISTICS PER TYPE OF DETERIORATION	UNION	INTERSECTION	TYPE OF PERCENTAGE	UNION	INTERSECTION
1) PROBABILITY OF DETECTING AFFECTED AREA	41.67%	100.00%	A) DETECTION IN RADAR ONLY (NY)	16.00%	28.00%
2) PROBABILITY OF DETECTING NON-AFFECTED AREA	69.23%	69.57%	B) DETECTION IN CORE ONLY (YN)	28.00%	0.00%
3) FALSE ALARM RATE OF DETECTING AFFECTED AREA	30.77%	30.43%	C) DETECTED IN BOTH (YY)	20.00%	8.00%
4) FALSE ALARM RATE OF DETECTING NON-AFFECTED AREA	58.33%	0.00%	D) AREA OF NO DETECTIONS (NN)	36.00%	64.00%
OVERALL CORRELATION RATE:	56.00%	72.00%	TOTALS:	100.00%	100.00%

FORMULAS USED FOR COMPUTING RESPECTIVE STATISTICS

1) C/(B+C)
2) D/(1-(B+C))
3) A/(1-(B+C))
4) B/(B+C)

Figure 6-8. Evaluation of distorted top mat rear echo as a discriminant for various indicators of deterioration--Shinning Creek bridge, Virginia.

the presence of delamination, and there was found to be a significant correlation. As previously discussed, this increase is due almost entirely to the presence of moisture in the concrete or moisture at the A/C interface. It was found that the A/C discriminant was very effective on many bridge decks. However, several disadvantages exist relative to its use including:

- This indicator is almost entirely moisture dependent and it is known that moisture alone is not a sufficient cause of rebar corrosion and subsequent delamination. Therefore, it is less directly connected with delamination.

- When actually measuring the amplitude of this signal, thin asphalt layers created erroneous predictions because of the superposition of the very strong surface echo with the weaker A/C echo.

- Varying thickness of asphalt layers also caused changes in the amplitude of this echo.

- Standing moisture on the bridge deck caused erroneous predictions.

Increase or Decrease in Rebar Echo

Rebar echo changes were observed in some of the bridges included in the study. The amplitude of the top rebars are normally variant, based on the position of the radar antenna relative to the rebars. A slight variation in the echo amplitude is normal for bridges with grid type reinforcing arrangements when the radar signal reflects from the transverse rebars. This is particularly true for the top layer of reinforcing bars where the antenna beamwidth is nondivergent. However, at the bottom reinforcing steel mat, the beamwidth is considerably broader, resulting in less effect from the transverse reinforcing steel bars, producing a steadier signal. Increases in rebar amplitude were observed in some of the bridges, and there was a correspondence between this discriminant and the occurrence of delamination. No significant correlation was observed between decrease in rebar echo and delamination at the top rebar. Actually, the echo caused by the rebar does not increase in amplitude, but rather the laminar fracture caused by a delamination algebraically sums with the echo from the rebar to yield a net increase in the echo in the region about the rebar. The effective rebar echo increase is actually caused by a laminar fracture and can be modeled as a laminar fracture plane in a homogeneous medium. This indicator was used with success in the detection of delaminations occurring at the bottom reinforcing steel in the I-87 Major Deegan Expressway bridge deck in the Bronx, New York.

Signal Distortion

The echo from the top reinforcing steel was found to be distorted in some cases when delamination was present. The echo distortion with respect to top reinforcing steel is described in detail in work performed by the Ontario Ministry of Transportation (1, 14-17). This indicator is predicated on a signature analysis technique. When the bridge deck concrete is in sound condition, a "W" type waveshape is present, comprising the region of signal between the A/C interface and the top reinforcing steel. When a delamination occurs, the "W" waveshape is distorted, and instead of a negative-positive-negative-positive slope existing, the slope of the signal becomes negative-positive, resembling a "V" shape. This discriminant is based on the same model that describes the I/A discriminant and also results from the superposition of the echo from the laminar fracture on the rebar echo. It is believed that very small delaminations will only produce a distortion of the rebar echo, whereas larger delaminations will cause an increase in the rebar echo. The main limitation of this discriminant results when the top reinforcing steel is close to the concrete surface, i.e., less than about 2 in. (5.08 cm) for a 1 ns pulse. In this case, the system resolution is insufficient to adequately separate the rebar echo from the A/C echo, and the characteristic "W" will not exist even if the concrete is sound. This delamination discriminant provides a direct indication of the delamination, and when the proper conditions exist, it is effective.

Decrease in Propagation Velocity

A decrease in propagation velocity through a material is related entirely to the dielectric of the material. When concrete possesses large amounts of moisture, its relative dielectric constant increases. A correlation exists between this occurrence and the presence of a delamination. However, its major shortcoming relates to its actual use. This discriminant involves monitoring a well-defined signal in the waveform, such as the deck bottom echo. Aside from being entirely dependent on moisture and not chloride, the major limitation results when severe signal attenuation takes place, making it impossible to distinguish the echo needed to measure the increase in transit time.

Increase in Signal Attenuation

Typically, under usual circumstances signal loss is an effect that is undesirable and efforts are usually made to improve and increase transmitted power to overcome this limitation. In bridge deck concrete, it was found that high levels of signal loss occurred with great

frequency when delamination and deteriorated concrete were present. The combination of moisture and chloride intrusion into the concrete creates a condition of very high material conductivity resulting in RF signal attenuation, which is easily detectable. The signal attenuation effect was also found to occur when wide vertical and laminar cracks were present in the concrete, probably due to complex scattering of the RF signal. One undesirable effect relative to this discriminant was its responsiveness to severe asphalt deterioration. Overall, the attenuation discriminant was found to be the most effective among those studied, and additional work was conducted with it to define optimum thresholds for delamination quantity prediction.

Delamination at the Top Reinforcing Steel

To summarize the results of actual field tests, it was found that the increase in attenuation (I/A) discriminant consistently appeared to be the most effective in the detection of delamination at the top reinforcing steel. This discriminant was found to be responsive to both moisture and chloride in the bridge deck concrete. Under very dry concrete conditions, and for delamination occurring in low permeability concrete, this discriminant was less effective due to lower conductivity in the concrete. The increase in A/C echo and decrease in P/V discriminants were also effective in many cases, although they were not as consistent or easily detectable over a wide sampling of bridge decks. As stated previously, these discriminants are dependent primarily on moisture and are less closely related to delamination than signal attenuation. The increase in rebar echo (I/R) discriminant was not very effective in top level delamination detection for most of the bridge decks, even though theoretically and experimentally it was predicted to be. The likely reason for this was that the delaminations encountered were small in size. Theoretically, thinner or smaller delaminations produce smaller reflections, and, since there is normally considerable variability in the top reinforcing steel echo due to the position of the antenna with respect to the transverse rebars, slight increases in the rebar echo due to delamination may not be perceived. The "W" discriminant has been shown to be effective in detection of top delamination. However, results suggest that this indicator should be utilized only during very dry concrete conditions or for delaminations occurring in low permeability concrete as a complement to the increased attenuation discriminant. Figures 6-9 through 6-12 show radar waveforms from both sound and delaminated areas of two representative bridge decks. Some of the aforementioned discriminants can be observed.

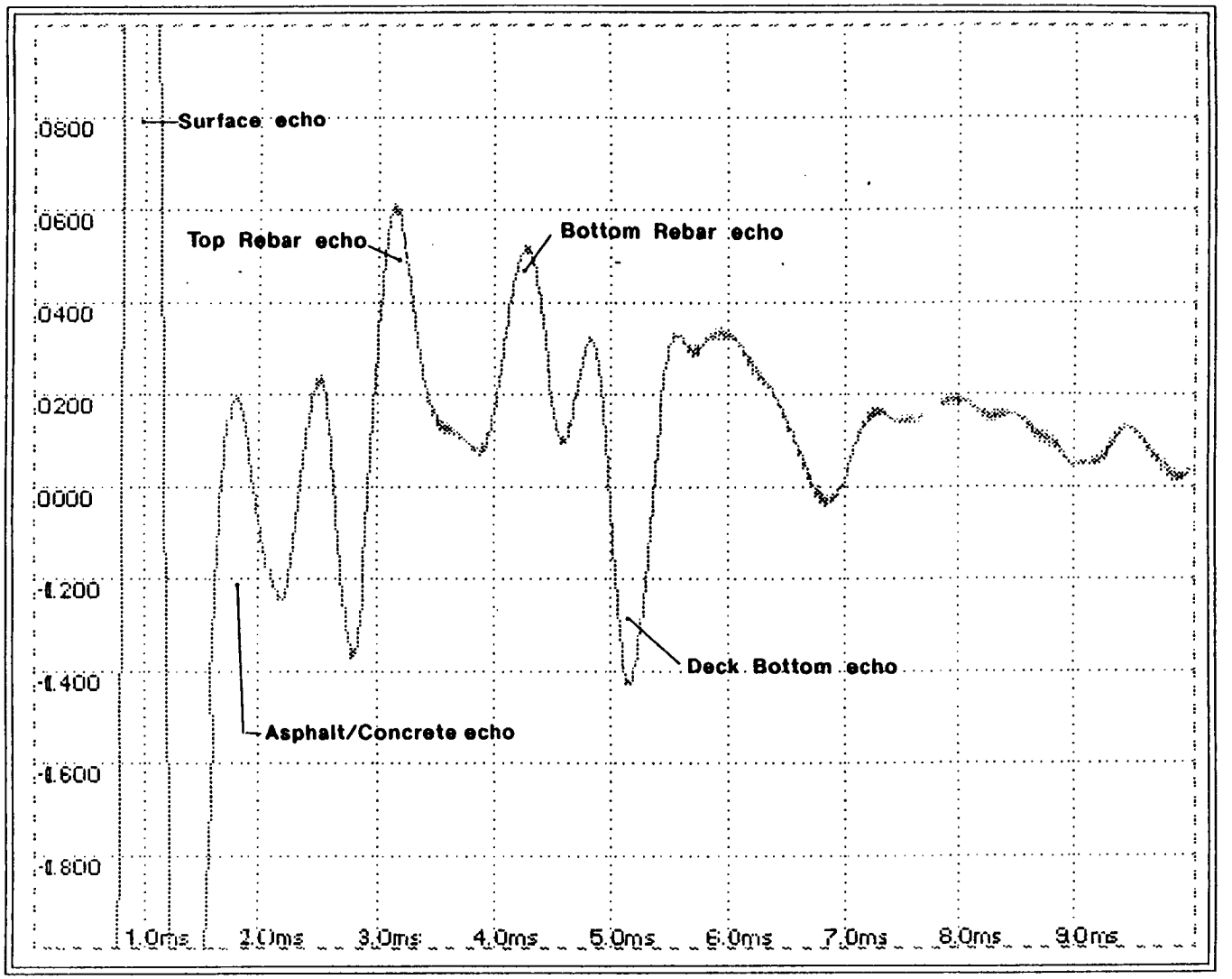

Figure 6-9. Radar waveform from I-91 Rockingham, Vermont bridge--sound concrete.

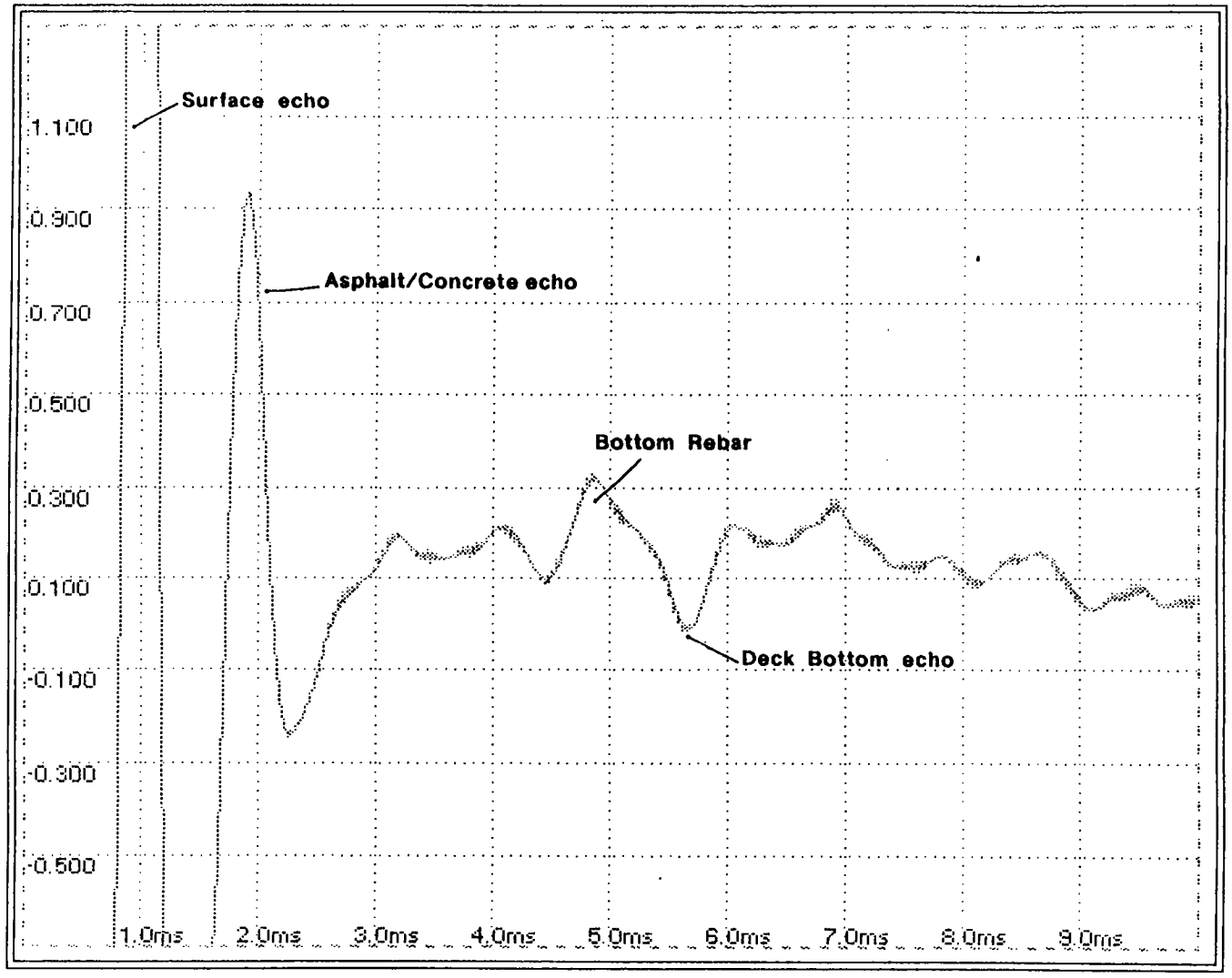

Figure 6-10. Radar waveform from I-91 Rockingham, Vermont bridge--delaminated concrete.

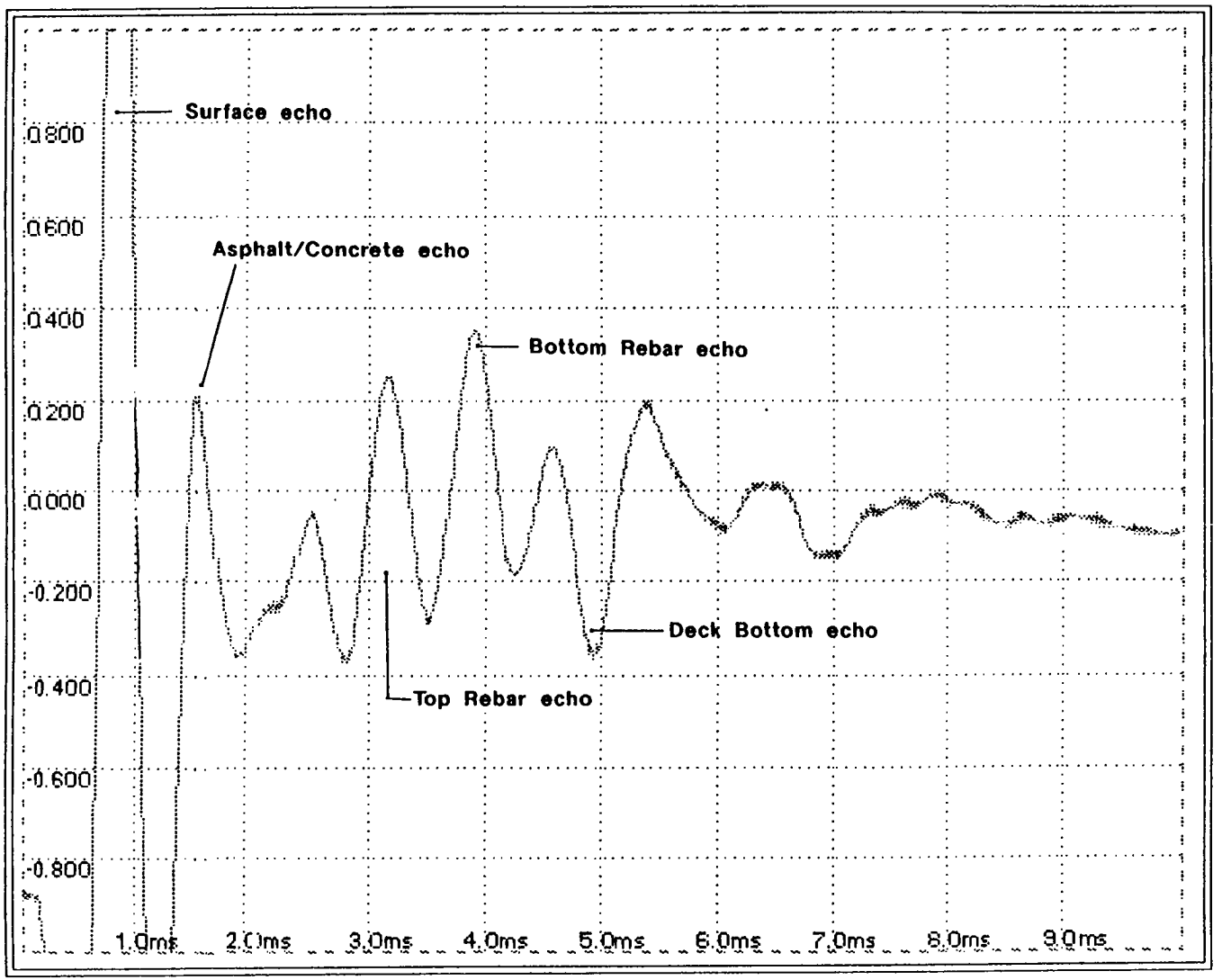

Figure 6-11. Radar waveform from Rt. 1 bridge over Nottoway Creek, Virginia--sound concrete.

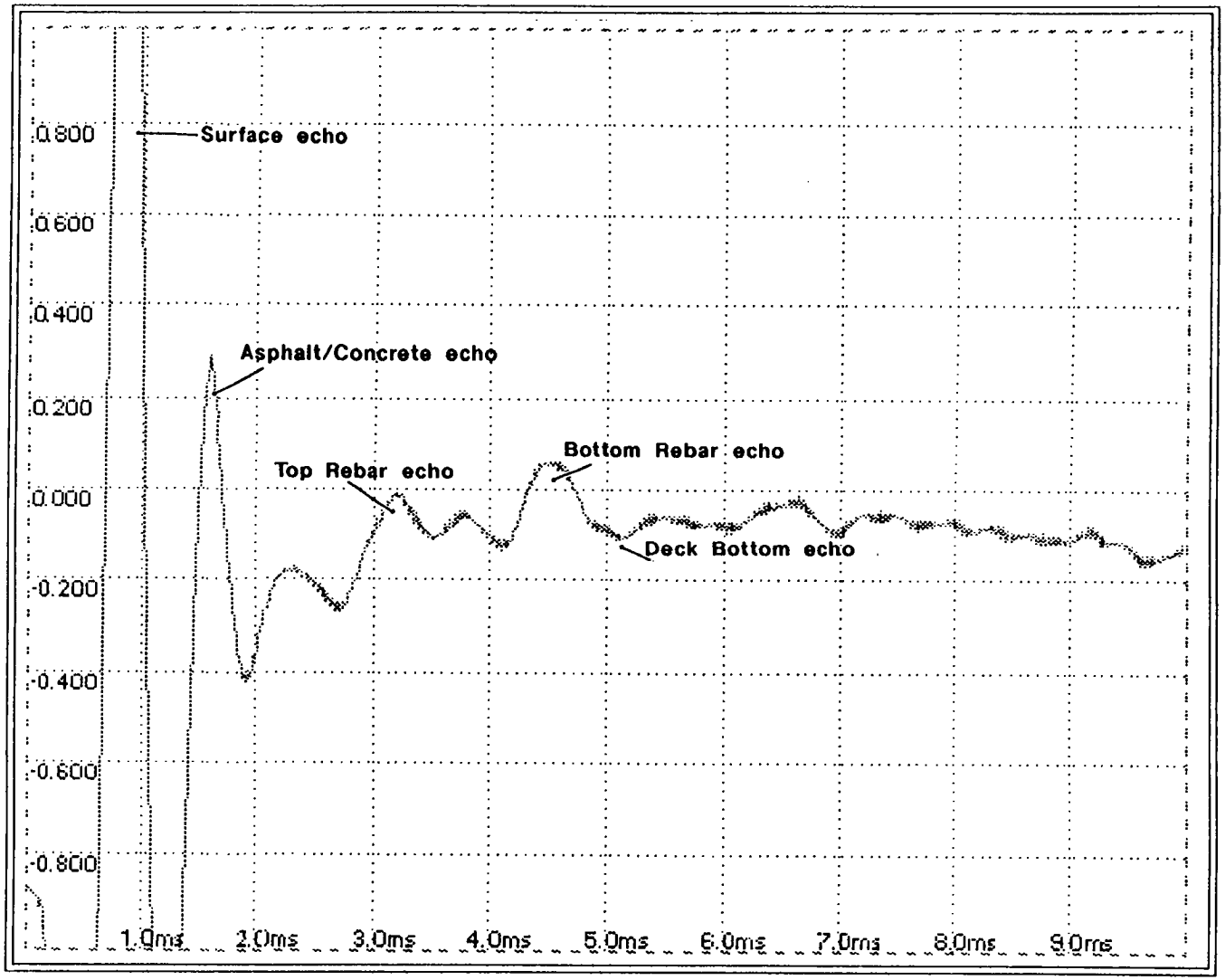

Figure 6-12. Radar waveform from Rt. 1 bridge over Nottoway Creek, Virginia--delaminated concrete.

Delamination at the Bottom Reinforcing Steel

Only limited field data were obtained with respect to bottom level delamination. A study was conducted on one bridge deck, the I-87 Major Deegan Expressway Bridge in the Bronx, New York. It was reported that significant bottom level delamination and spalling had occurred. It is speculated that two cases will exist, relative to the expected radar waveform, depending on the type of deterioration present. Delamination at the bottom reinforcing steel can be modeled as an air gap in an homogeneous medium. It is expected that the signal amplitude of the bottom rebar will increase in the presence of delamination, in accordance with the model. For spalled areas, where the bottom reinforcing steel is exposed, it is believed that the echo from the bottom steel will diminish, since the deck bottom echo and the echo from the reinforcing steel will be effectively superimposed. Correlation data were gathered by NYSDOT in the form of soundings of the bottom of the deck and visual observation of the spalled areas. The test results for eight locations, comparing radar and ground truth, supported the hypothesis relative to bottom delamination and spalling. Six of eight test locations were predicted correctly, yielding an overall correct rate of estimation of 0.75. The overestimation and underestimation rate were each 0.125. All four delaminated areas were predicted correctly with no overestimation or underestimation, whereas only two of four spalled areas were correctly identified. The conclusion, based on this limited sampling of data from one bridge deck, suggests that radar can be utilized for detection of deck bottom delamination. Bottom spalling can also be detected, however, with lower accuracy rates. The discriminants were computer-detected and plotted onto maps showing longitudinal radar scan passes versus distance. Results from the NYSDOT inspection of the eight radar detected locations are presented in Table 6-1. A map showing a portion of the deck containing six of the eight areas detailed in Table 6-1 is presented in Figure 6-13. It is based on the two deterioration discriminants discussed, increase in bottom rebar echo and decrease in bottom rebar echo. The areas examined by NYSDOT have been outlined. Hard copy output of actual radar waveforms were produced to illustrate these effects, as shown in Figures 6-14 through 6-16. Figure 6-14 shows the waveform for pass K at 45 ft (13.7 m), a sound area. Notice the magnitude of the bottom rebar echo. Compare Figure 6-14 with Figure 6-15, a delaminated region located at 27 ft (8.2 m) of pass K. The bottom rebar echo at the delaminated area is obviously larger than that at the sound area, as predicted. Figure 6-16 shows a waveform for a spalled area located at 11.9 ft (3.6 m) on pass R. Comparing this with Figure 6-14 reveals a significant decrease in bottom rebar echo--again, as predicted. A decrease in the echo from the bottom reinforcing steel may also occur from chloride-related signal attenuation in the concrete. Hence, this discriminant must be used carefully for detection of bottom spalling, since it is not unique.

Table 6-1. Radar prediction of delamination and spalling versus ground truth.

Site Number	Lontiduginal Range (Ft)*	Transverse Range (Pass)	Comments (1) NYSDOT Findings (2) Radar Findings
1	8-37	D-H	(1) Visible delamination of deck bottom (2) Prediction of bottom delamination
2	14-36	K	(1) Visible delamination of deck bottom (2) Prediction of bottom delamination
3	8-20	N-O	(1) Bottom scaling and reinforcing bars exposed about 25 percent beyond radar prediction (2) Prediction of bottom spalling
4	8-20	R-S	(1) Bottom scaling and reinforcing bars exposed about 25 percent beyond radar prediction (2) Prediction of bottom spalling
5	60-72	J-O	(1) "Hollow" area marked (delaminated) (2) Prediction of bottom delamination
6	108-122	O-S	(1) "Hollow" area marked (delaminated) (2) Prediction of bottom delamination
7	130-146	O-S	(1) Visible scaling (2) No prediction of spalling
8	308-350	J-S	(1) Few visible scaled areas (2) Prediction of bottom spalling in areas

*Note: 1 ft = 30 cm (approximately)

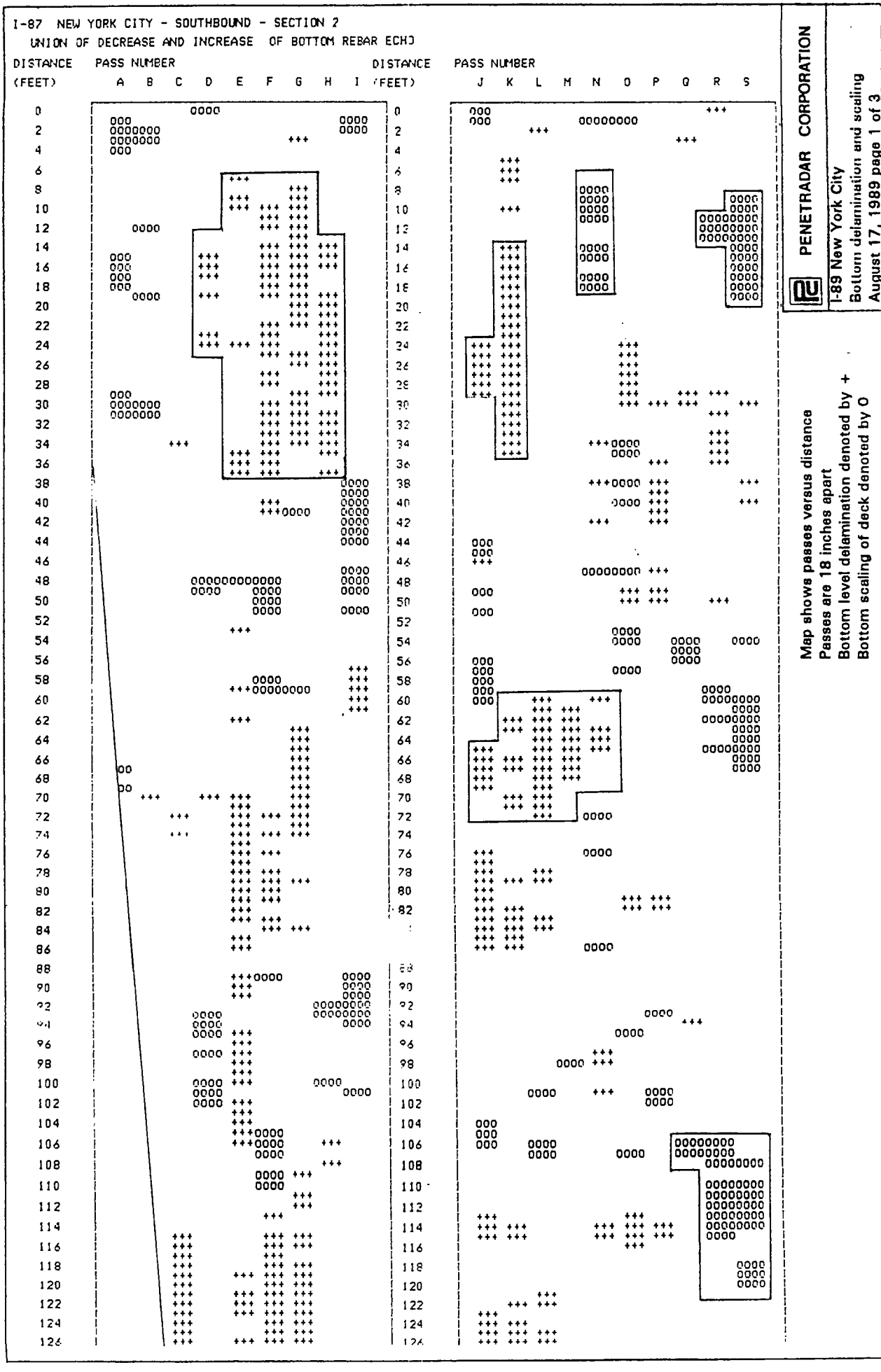

Figure 6-13. Map of portion of the Major Deegan Expressway bridge showing locations of radar detected bottom delaminations and spalls and ground truth.

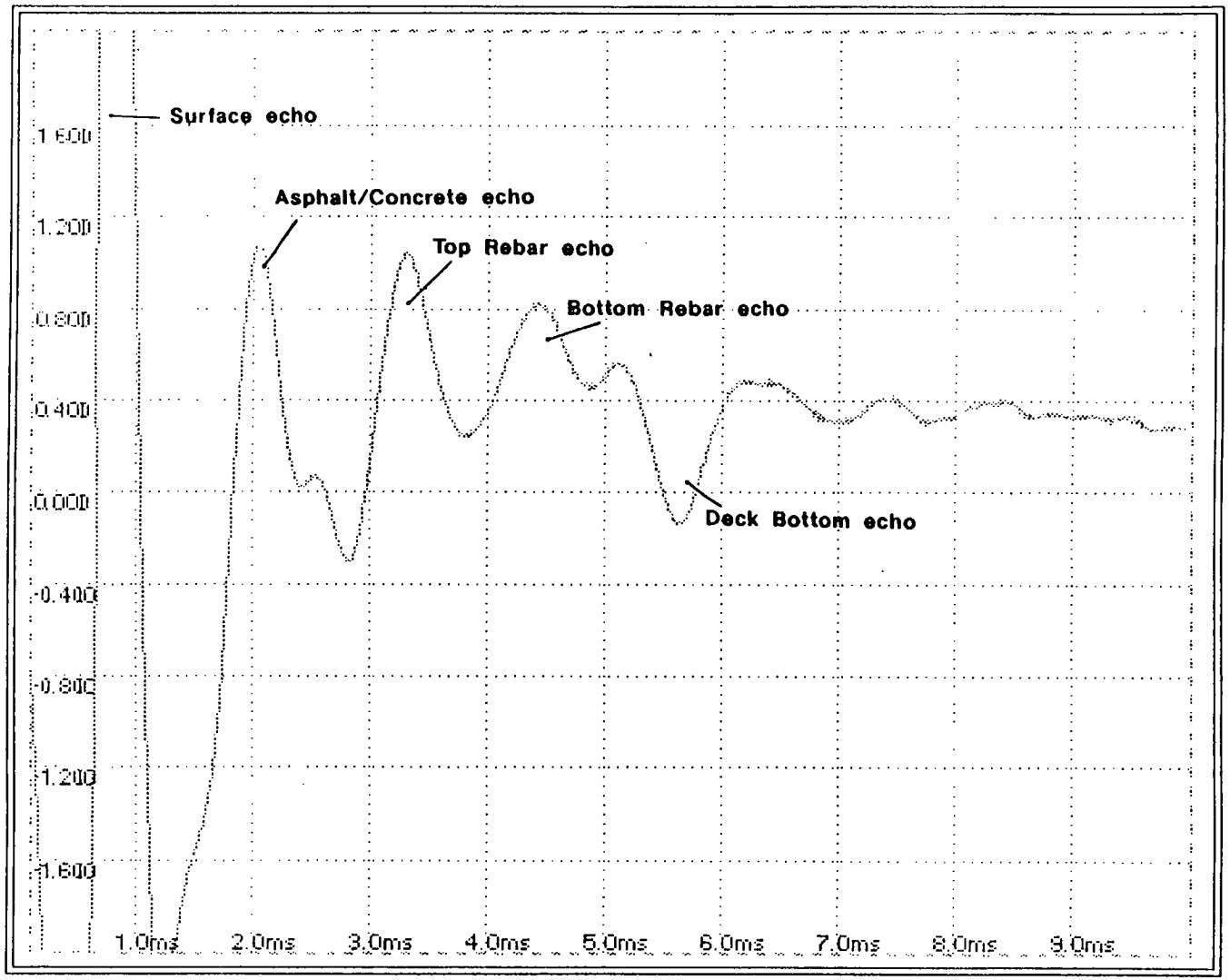

Figure 6-14. Radar waveform from I-87 bridge in New York--sound concrete, Pass K--45 ft (13.7 m).

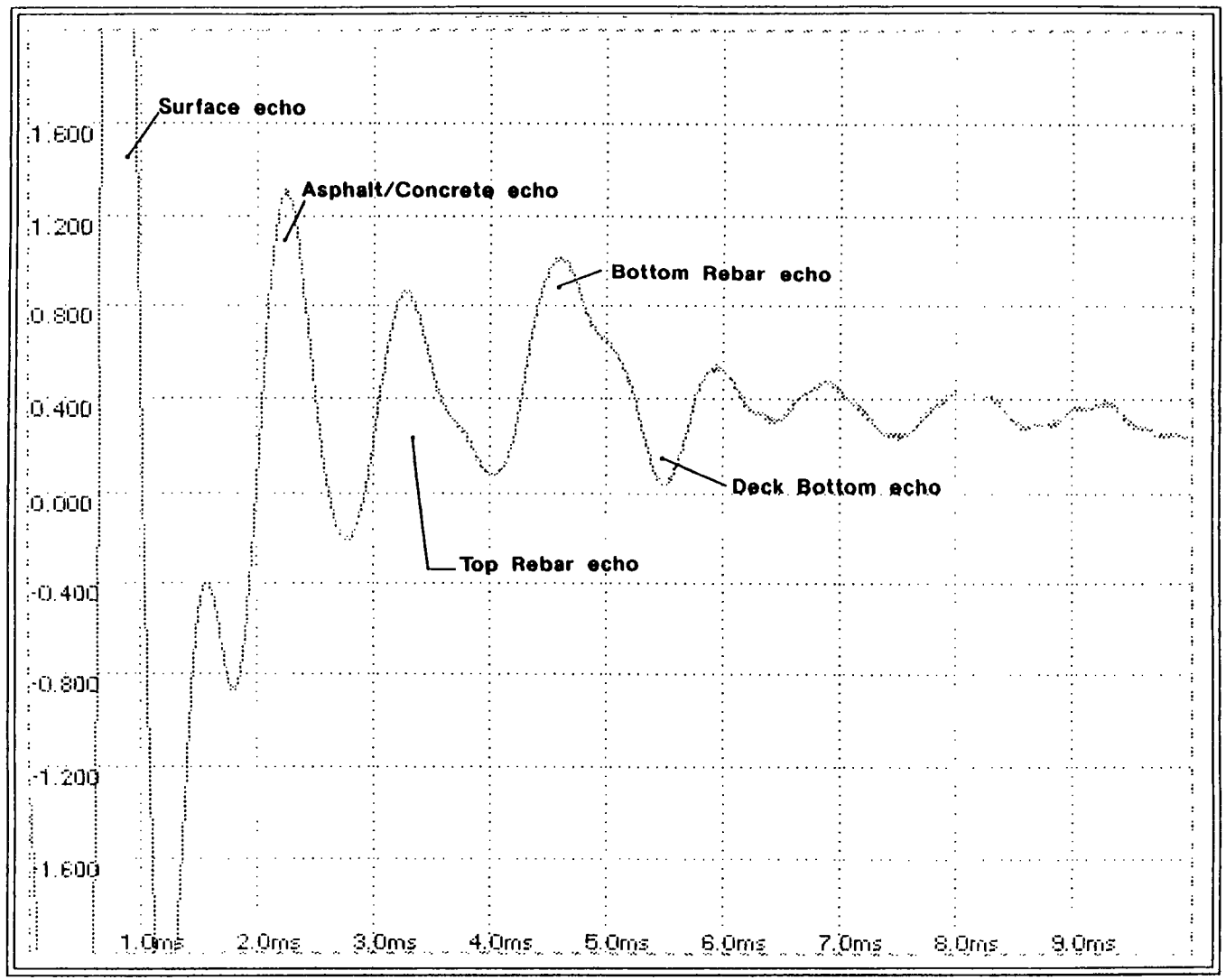

Figure 6-15. Radar waveform from I-87 bridge in New York--soffit delamination, pass K--27 ft (8.24 m).

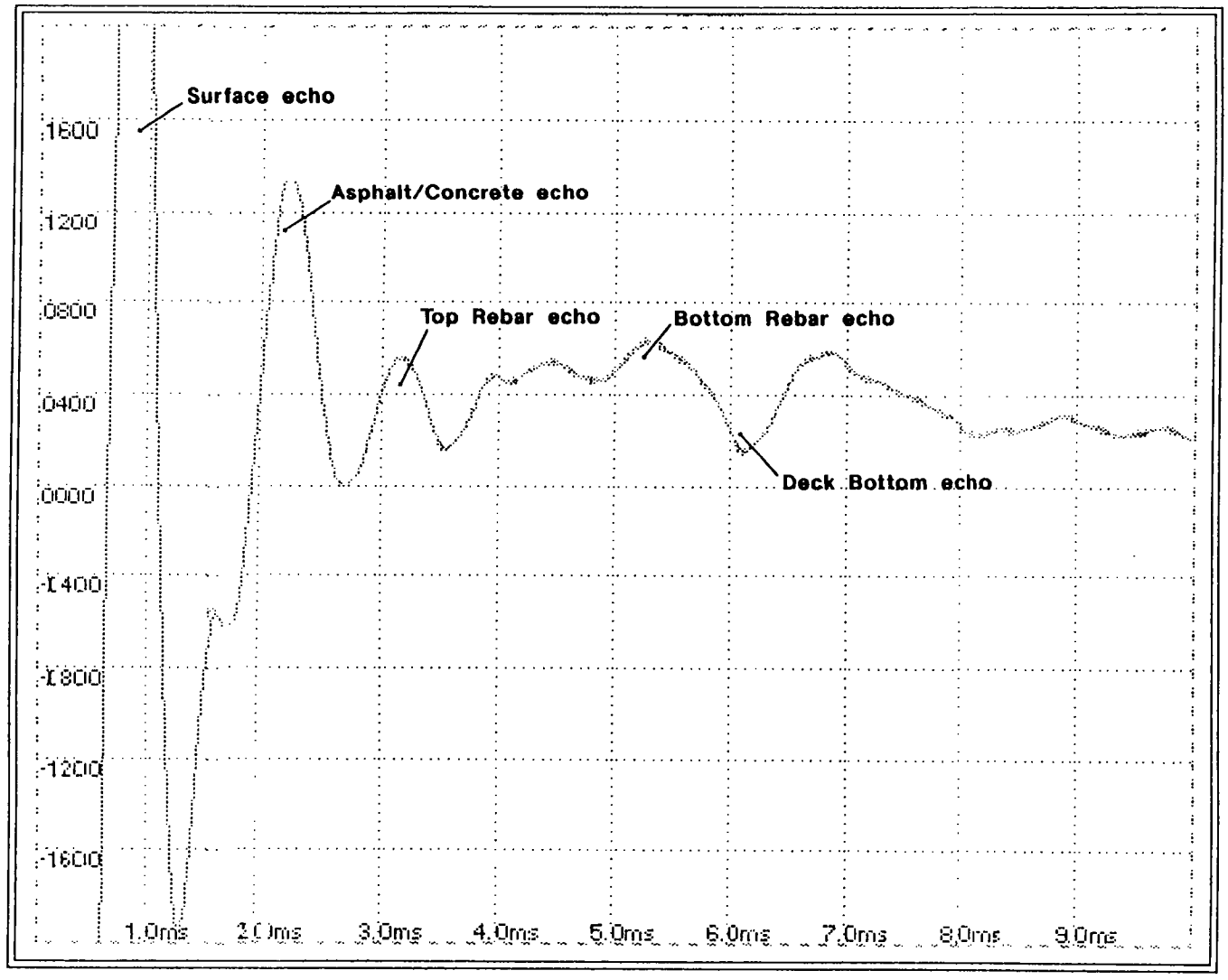

Figure 6-16. Radar waveform from I-87 bridge in New York--spall on deck bottom, Pass R, 11.9 ft (3.63 m).

Selection of Optimal Deterioration Discriminant

Relative to the objective of detecting delamination at the top reinforcing steel, the attenuation discriminant provided optimum results with respect to accuracy and reliability over a large sampling of bridge decks under normal moisture conditions. Dry concrete conditions allow the use of the "W" discriminant for delamination detection, provided that sufficient concrete cover over the reinforcing steel is present. For delamination at the lower mat of reinforcing steel, the optimum discriminant is an increase in the echo from the lower layer of reinforcing steel.

Repair Quantity Estimation

One objective of bridge condition assessment is the accurate estimation of repair quantities. The results of laboratory experimentation and analytical modeling have suggested that the radar signal attenuation discriminant would be most suitable for top reinforcement delamination detection. Field tests on bridge decks using this discriminant confirmed this assumption by consistently yielding the highest detection rate and the lowest false alarm rate relative to the delamination detection in a wide variety of cases. However, in order to make an assessment of bridge deck repair quantity, this discriminant must be quantified (how much signal attenuation is necessary to accurately reflect the actual quantity of delamination). With any nondestructive test method there is a degree of accuracy in detection as well as a false alarm rate. When radar results are compared to ground truth results, there are four possibilities that can exist with respect to the two data sets. These possibilities include:

1. A true detection of deterioration, where the deteriorated area detected by radar is also detected by ground truth;

2. An overestimation, where an area was detected by radar, but not by ground truth;

3. An underestimation, where an area was detected by ground truth and not by radar; and

4. A true detection of sound areas, the area not detected by radar or by ground truth corresponding to nondeteriorated areas.

If it is assumed that the ground truth data is correct, then the accurate deterioration estimation amount is 1 + 3. The information provided by radar is actually the amount

1 + 2, and in situ its accuracy is not known. In order to utilize any nondestructive method for effective deterioration quantity estimation, the amount detected by the device must equal the amount actually deteriorated, therefore, 1 + 3 = 1 + 2 or more simply 3 = 2. In other words, the overestimation rate by radar must equal the underestimation rate in order to estimate the correct deterioration quantity.

When applied to the attenuation discriminant, it can be seen that two extreme cases can exist. A very low attenuation threshold will result in a high overestimation rate and a low underestimation rate, whereas a high attenuation threshold will result in the opposite. Therefore, the problem is the determination of the proper attenuation threshold whereby the underestimation and overestimation rates are equal.

In order to estimate the proper attenuation threshold, it was necessary to compare the magnitude of the radar waveform from known deteriorated areas with known sound areas while the condition above is satisfied, i.e., the underestimation and overestimation rates are equivalent. In this manner we are actually determining the increase in signal attenuation in a deteriorated area relative to the normal attenuation occurring in the concrete deck. To find the nominal attenuation in the bridge deck concrete, a waveform is located where signal strength is at a maximum. All other waveforms are then normalized with respect to this waveform. All waveforms from each of the bridge decks were compared to several attenuation thresholds until the overestimation/underestimation criterion was met. At this point the optimum attenuation threshold was defined.

Two types of thresholds were considered for deterioration detection: a fixed threshold and a variable threshold. The fixed thresholding method uses a fixed value which is compared with the radar waveforms. The variable threshold method develops a threshold based on the average signal value multiplied by a fixed fractional value. There are advantages and disadvantages for each type of threshold. Specifically, it was found that the fixed threshold method was not as effective on bridge decks where attenuation levels for sound concrete varied significantly. Similarly, it was found that the variable threshold method was not as effective on bridge decks where significant portions of the deck exhibited high attenuation, since this eventually affects the threshold. In most cases, the fixed threshold method was most effective, primarily because radar data acquisition was conducted under relatively stable conditions (moisture levels were consistent throughout the deck). Consistent moisture levels means that there is no standing moisture or visibly wet areas on the deck. The variable attenuation threshold, however, was effective in locating deteriorated areas and, as an illustration, was used quite effectively in the first test on bridge 62640 in New York State. Excessive moisture and wet particulate debris were observed along the curb region of this particular deck, resulting in large overestimation of deterioration quantity using the fixed

threshold. The variable threshold method was able to compensate for this. In practice, however, radar testing of bridge decks during conditions of excessive moisture and where there are concentrations of wet antiskid material or other debris along the curbs should be avoided.

Table 6-2 shows the results from 11 bridge decks where the delamination prediction rate for radar is similar to the ground truth rate. In order to determine the correct attenuation level, the echo from the deck bottom was measured. The first column shows the ratio of the echo from what is considered a sound region of concrete deck to the emitted signal amplitude for each respective bridge deck. The second column gives the ratio of the echo from the deck bottom to the emitted signal amplitude (where the overestimation/underestimation criterion is met). The last column shows the total attenuation change in the concrete.

The mean value for the sound deck bottom echo versus emitted signal is -25.5 dB with a standard deviation of 3.03 dB. The sound deck echo ratios for all of the bridges were close in range indicating that the deck attenuation from sound areas was similar regardless of slight differences in thickness, type of asphalt overlay, moisture condition, and geographic location. There was a tendency, however, for normal deck attenuation in the Virginia bridges to be slightly lower than attenuation in the New York and Vermont bridges. This is probably due to lower overall salt exposure in southern bridges. The normalized echoes from the deck bottoms, at the threshold corresponding to the optimum overall delamination detection rate, were also similar. The mean value was -33.8 dB with a standard deviation of 3.25 dB. The change in attenuation ranged from 5.5 dB to 11.2 dB, however, most of the values ranged between 7 dB and 9 dB. The mean value for the increase in bridge deck attenuation for this sample was -8.3 dB with a standard deviation of 1.46 dB. This is for bridge deck thicknesses between approximately 7 and 8 in. (18 to 20 cm). The only apparent outliers in these data are from bridge 62640, which was tested twice, under wet and dry conditions. In each of these cases, extreme threshold values were obtained. This suggests that dry conditions require a slight lowering of the attenuation threshold to increase detections, whereas high moisture conditions require raising the threshold to decrease detections. The correction factor necessary to compensate for deck moisture is not known. However, based on the threshold variations in bridge 62640, a factor of +/- one standard deviation about the mean threshold is probably not unreasonable for optimizing predictions relative to moisture variations. Therefore, threshold values of -6.8 dB and -9.8 dB would likely yield better predictions for lower and higher moisture conditions, respectively, than the average value of -8.3 dB.

Table 6-2. Signal attenuation threshold for delamination at top reinforcing steel.

Bridge Deck	"Sound" deck bottom echo relative to emmitted signal (dB)	Bottom echo at delamination threshold relative to emmitted signal (dB)	Δattenuation (difference between column 1 and column 2) (dB)
62640 Kennedy 1st	-27.9	-39.1	-11.2
62640 Kennedy 2nd	-25.8	-31.3	-5.5
950 DX W Ripley	-26.9	-33.8	-6.9
950 DX E Ripley	-26.9	-35.5	-8.4
I-91 Rockingham	-26.9	-35.3	-8.6
RT 1 Nottway	-27.1	-35.9	-8.8
RT 1 Shinning Creek	-20.7	-29.7	-9.0
RT 1 Meherrim	-28.3	-36.8	-8.5
RT 220 Blackwater	-22.9	-30.9	-8.0
RT 211 Shenandoah	-19.5	-28.7	-9.2
RT 60 Dunkirk	-27.5	-34.7	-7.2
$\overline{X}$	-25.5	-33.8	-8.3
σ^{n-1}	3.03	3.25	1.46

Using the attenuation threshold of -8.3 dB (0.385) and comparing this to the calculated increase in attenuation results in an average error in radar prediction of +/- 11.2 percent with respect to delaminated area as determined by ground truth methods (chain drag, core sample, and actual repair quantities). (This was derived after elimination of the data from bridge 62640 in New York from the sample.) Therefore, under relatively normal and uniform bridge deck moisture conditions it can be expected that radar will make delamination predictions within +/- 11.2 percent of the ground truth quantities at the -8.3 dB attenuation threshold.

7

Summary and Conclusion

Short pulse GPR has been investigated and developed as an effective method for detection of delamination at the top reinforcing steel and determination of delamination removal quantities based on the results of analytical models and laboratory and field experimentation. The successful radar detection of delamination at the bottom reinforcing steel layer also was demonstrated. Extensive analytical RF modeling of bridge deck concrete was conducted, with the addition of reinforcing steel and elements commonly found within, including water and chloride. The model was extended for the cases of concrete delamination when the concrete is dry or when it is moist. It was determined that radar is theoretically capable of detecting the delamination air gap directly when the concrete is dry and relatively low-loss conditions exist. Similarly, under high-loss conditions, it was determined that radar could detect delamination by measurement of the causes of delamination (i.e., water and chloride) through a signal attenuation discriminant. A field test program was carried out on 22 bridge decks in Virginia, New York, and Vermont. The specimen bridge decks were examined by radar, and the identification of increased signal attenuation as the optimum delamination discriminant verified previous analytical models. Extensive analysis of the gathered field data was performed, permitting quantification of an attenuation threshold, which detects delamination at the top reinforcing steel and accurately determines actual repair quantities. Delamination at the bottom reinforcing steel is detected in accordance with the previously developed model for a planar air gap in a homogeneous material. Advanced radar data acquisition and signal processing equipment were developed for this project, employing specially designed electronic hardware, 80486-based industrial computer equipment, and custom software, which utilized the results of the delamination detection research.

Other results of this research include a possible means for the utilization of radar for the detection and measurement of chloride in concrete as well as the detection of highly permeable concrete.

Problems remain, however, relative to the use of radar in the case of dry concrete where reinforcing steel is close to the A/C interface. Moisture- and chloride-based delamination discriminants are less effective here, and waveform distortion processing discriminants, which are normally used in these instances, are also limited. Additional work is necessary in defining the conditions under which bottom (soffit) delaminations are detectable as well as the corresponding optimum detection threshold for accurate quantity estimation of bottom delaminations.

Overall, this research effort has yielded a means for the detection and quantity estimation of delamination at the top reinforcing steel in asphalt-covered bridge decks along with improved data acquisition and signal-processing hardware for effective decision making relative to bridge deck repair and rehabilitation.

References

1. Manning, D.G. and F.B. Holt. *Detecting Deterioration in Asphalt-Covered Bridge Decks.* Ontario, Canada: Research and Development Branch, Ontario Ministry of Transportation and Communications, September 1982.

2. Clemena, G.G. *Evaluating of Overlaid Bridge Decks with Ground-Probing Radar.* Report No. 80-WP21. Charlottesville, VA: Virginia Highway and Transportation Council, 1980.

3. Penetradar Corporation *Interstate Bridge Deck Pavement Radar Tests.* Technical Note PTN-002. Niagara Falls, N.Y.: Penetradar Corporation.

4. Alongi, A.V. *Radar Examination of Conditions of Two Interstate Highway Bridge Decks.* Niagara Falls, New York: Penetradar Corporation, 1973.

5. Maser, K.R. *New Technology for Bridge Deck Assessment.* Phase II. Final Report. Cambridge, MA: New England Transportation Consortium Bridge Deck Technical Committee, 1990.

6. Maser, K.R. *New Technology for Bridge Deck Assessment.* Phase I, Volume I and II. Cambridge, MA: New England Transportation Consortium Bridge Deck Technical Committee, 1989.

7. Cantor, T. and C. Kneeter. *Radar as Applied to Evaluation of Bridge Decks.* Transportation Research Record No. 853. Washington, D.C.: Transportation Research Board, 1982.

8. Joyce, R.P. *Rapid Non-destructive Delamination Detection.* FHWA/RD-85/051. Washington, D.C.: Federal Highway Administration, Office of Engineering and Highway Operations Research and Development, April 1985.

9. Alongi, A.V. and A.J. Alongi. *Design Consideration for a Short Pulse, High Resolution Radar.* Technical Report PTR-0677. Niagara Falls, N.Y.: Penetradar Corporation, June 2, 1977.

10. Johnson, W.C. *Transmission Lines and Networks.* McGraw-Hill Electrical and Electronic Engineering Series. New York: McGraw-Hill, 1950.

11. Bechtel, M.E. and A.V. Alongi. *Reflection from Wire-mesh Shielding Structures*. Technical Report SC-1. Niagara Falls, N.Y.: Penetradar Corporation, August 25, 1976.

12. Alongi, A.V., T.R. Cantor, C.P. Kneeter, and A.J. Alongi. *Concrete Evaluation by Radar Theoretical Analysis*. Transportation Research Record 853. Washington, D.C.: Transportation Research Board, 1982.

13. Alongi, A.J. and A.V. Alongi. *Synthesis of Radar Echoes From Multilayers*. Technical Report PTR-010680. Niagara Falls, N.Y.: Penetradar Corporation, June 10, 1980.

14. Chung, T. and C.R. Carter. *Upgrading of DART Software to 386 Computer Specifications*. Hamilton, Ontario, Canada: Communications Research Laboratory, McMaster University, December 1990.

15. Chung, T. and C.R. Carter. *Radar Signal Enhancement for DART*, Hamilton, Ontario, Canada: Communication Research Laboratory, McMaster University, June 1989.

16. Chung, T. and C.R. Carter. *Signature Analysis of Radar Waveforms Taken on Asphalt Covered Bridge Decks*. Hamilton, Ontario, Canada: Communications Laboratory, McMaster University, June 1984.

17. Manning, D.G. and F.B. Holt. *The Development of D.A.R.T. (Deck Assessment by Radar and Thermography)*. Ontario, Canada: The Research & Development Branch, Ontario Ministry of Transportation and Communications, November 1985.